A seven-residue deletion in PrP leads to generation of a spontaneous prion formed from C-terminal C1 fragment of PrP

Carola Munoz-Montesino, Djabir Larkem, Clément Barbereau, Angélique Igel-Egalon, Sandrine Truchet, Eric Jacquet, Naïma Nhiri, Mohammed Moudjou, Christina Sizun, Human Rezaei, et al.

JBC Papers in Press. Published on August 11, 2020 as Manuscript RA120.014738
The latest version is at https://www.jbc.org/cgi/doi/10.1074/jbc.RA120.014738

A seven-residue deletion in PrP leads to generation of a spontaneous prion formed from C-terminal C1 fragment of PrP

Carola Munoz-Montesino [1§#], Djabir Larkem [1§], Clément Barbereau [1‡], Angélique Igel-Egalon [1], Sandrine Truchet [1], Eric Jacquet [2], Naïma Nhiri [2], Mohammed Moudjou [1], Christina Sizun [2], Human Rezaei [1], Vincent Béringue [1], and Michel Dron [1*]

[1] Université Paris-Saclay, INRAE, UVSQ, VIM, 78350, Jouy-en-Josas, France

[2] Institut de Chimie des Substances Naturelles, CNRS, Université Paris Saclay, 91190, Gif-sur-Yvette, France

[§] These authors have equally contributed to this work
[#]Present address: Departamento de Fisiología, Facultad de Ciencias Biológicas, Universidad de Concepción, Chile
[‡]Present address: MMDN, Univ. Montpellier, EPHE, INSERM, U1198, F-34095 Montpellier, France

*Corresponding author: Michel Dron

E-mail: michel.dron@inrae.fr

Running Title: Spontaneous emergence of a new mutant prion in cell culture

Keywords: prion, prion diseases, structural biology, infection, mutant, cell culture, protein stability, protein aggregation, proteinase, recombinant protein expression

Abstract

Prions result from a drastic conformational change of the host-encoded cellular prion protein (PrP), leading to the formation of beta-sheet-rich, insoluble and protease-resistant self-replicating assemblies (PrP^{Sc}). The cellular and molecular mechanisms involved in spontaneous prion formation in sporadic and inherited human prion diseases or equivalent animal diseases are poorly understood, in part because cell models of spontaneously-forming prions are currently lacking. Here, extending studies on the role of H2 alpha-helix C-terminus of PrP, we found that deletion of the highly conserved $_{190}$HTVTTTT$_{196}$ segment of ovine PrP led to spontaneous prion formation in the RK13 rabbit kidney cell model. On long-term passage, the mutant cells stably produced proteinase-K resistant, insoluble and aggregated assemblies that were infectious for naïve cells expressing either the mutant protein or other PrPs with slightly different deletions in the same area. The electrophoretic pattern of PK-resistant core of the spontaneous prion (Δ^{Spont}) contained mainly C-terminal polypeptides akin to C1, the cell-surface anchored C-terminal moiety of PrP generated by natural cellular processing. RK13 cells expressing solely Δ190-196 C1 PrP construct, in absence of the full-length protein, were susceptible to Δ^{Spont} prions. Δ^{Spont} infection induced the conversion of the mutated C1 into a PK-resistant and infectious form perpetuating the biochemical characteristics of Δ^{Spont} prion. In conclusion this work provides a unique cell-derived system generating spontaneous prions and provides evidence that the 113 C-terminal residues of PrP are sufficient for a self-propagating prion entity.

Introduction

Mammalian prions are responsible for transmissible spongiform encephalopathies (TSE) in both humans and animals. Prions result from the misfolding of the host-encoded prion protein (PrP). Under its normal conformation, the cell surface GPI-anchored PrP (PrP^{C}) presents a globular domain containing three alpha-helices and two short antiparallel beta strands, preceded by an unstructured N-terminal part (1,2). In contrast, prions are made from assemblies of beta-sheet-rich, insoluble, aggregative and mostly partially protease-resistant PrP conformers called PrP^{Sc} in reference to their original identification in scrapie-infected sheep (3). Prion replication appears to proceed by conversion of the normal protein through templated polymerization (4), which explains not only their propagation in tissues but also their intra- or interspecific infectivity. The high-resolution structure of PrP^{Sc} is not yet resolved, due to inherent difficulties to produce large amounts of purified insoluble assemblies that may nonetheless have some intrinsic heterogeneity with respect to size. Several amyloid models were proposed and coexistence of different candidate structures has even been suggested (5-7).

The two-third C-terminal part of PrP forming the protease-resistant core of PrP^{Sc}, the C2 fragment, constitutes the domain necessary and sufficient for prion replication (8,9). Prion strains are identified by their specific biochemical and/or neuropathological features in the same infected host-species (10,11). Strains result from structural differences in three-dimensional or quaternary structure of PrP^{Sc}. The N-terminal border of the C2 fragment is strain-dependent and can vary around amino acid positions 80 to 100.

A C-terminal fragment called C1 results from the natural cleavage of PrP^{C} by a cellular protease at the alpha cleavage site, which is between residues 110 and 111 of human PrP (8,12). C1 is thus smaller than C2 and considered so far too short to be converted into prions although it encompasses the structured globular domain of the full-length PrP^{C} and is also present at the cell surface (13,14).

Prions can emerge spontaneously as in sporadic cases of human Creutzfeldt-Jakob disease (CJD), that is without evidence of infection or contamination. In this context, prion generation requires at first the formation of nuclei stable enough to initiate the polymerization process, which is expected to be a slow and rate-limiting step (15). Indeed, spontaneous prion disease is a rare event, the prevalence of sporadic CJD being of approximately 1.5 case per million and per year worldwide. Mutations in PrP can favor PrP spontaneous conversion into prions. Indeed, more than 30 mutations responsible for inherited human prion diseases, including genetic CJD, Gerstmann-Sträussler-Scheinker syndrome (GSS) or Fatal Familial Insomnia, were identified and these

dominant allelic mutations usually show a high penetrance (16). Disease-causing mutations might favor partial unfolding or transient denaturation of PrP^{C}, which are required for refolding into PrP^{Sc}, and might also increase stability of initial PrP^{Sc} seeds.

The cellular and molecular processes underpinning or preventing spontaneous prion generation remain poorly understood. Transgenic mouse models of spontaneous prion formation have proven difficult to obtain. This was achieved for human or mouse PrP bearing some mutations (17,18). Hallmarks of the disease were not always reproduced in mice and intriguingly in several instances, prions showed a rather low resistance to protease digestion (19). Prions spontaneously formed in mice overexpressing either anchorless mouse PrP or I109 allele of bank vole PrP (20,21). Currently, no cellular model for spontaneous prion formation has been reported. Toward this goal we focused here on an intriguing highly conserved threonine rich region of the alpha-helix H2 associated with several disease-causing mutations in human PrP (22). In a recent work, we demonstrated that deletion of the cluster of four threonines in the alpha-helix H2 C-terminus has no or marginal effect on ovine prions replication in RK13 cells expressing ovine PrP (23,24). We now show that specific deletion of the larger H2 C-terminal segment HTVTTTT, that removes three additional residues, causes the spontaneous conversion of the mutant ovine PrP into a new type of prion. This prion exhibits a main protease-resistant core shorter than usual, of C1 size, which was able to infect naïve RK13 cells expressing the mutant C1 segment alone. The potential importance of H2 C-terminus for maintenance of normal PrP^{C} conformation in the cell, the specificities of the new mutant prion and the surprising conversion of the homologous mutant C1 fragment into a prion entity are discussed.

Results

Δ190-196 deletion does not alter the overall structure of PrP but reduces its stability

We focused here on Δ190-196 ovine PrP (VRQ allelic variant), a mutant PrP with a specific deletion of seven amino acids at the end of helix H2 (Fig. 1). We previously reported that a larger deletion of the H2 C-terminus (Δ190-197) did not have a major impact on the structure of the protein, leaving intact the spatial organization of the three alpha helices in the globular domain of PrP (23). As with Δ190-197 PrP, structural analysis of recombinant Δ190-196 PrP by circular dichroism indicated a conservation of the overall alpha helical content compared to wild-type (WT) PrP (Fig. 2A). This is in agreement with NMR analysis of the segment 113-214 of Δ190-196 PrP ($C1_{113}$), which contains the entire sequence of the structured domain and is an equivalent to the natural C1 fragment studied hereinafter. The large dispersion of amide chemical shifts observed in the ^{1}H-^{15}N HSQC spectrum of $^{15}N^{13}C$-labeled mutant $C1_{113}$ indicated that it maintained a globular core, in addition to its unstructured N-terminal region (Fig. 2B). Moreover, comparison with the spectra of Δ193-196 and Δ190-197 mutant PrPs previously obtained (23,24) versus WT PrP showed that chemical shift perturbations followed a similar trend, confirming that the structure of the core domain of Δ190-196 $C1_{113}$ is structurally close to those of other mutants (Fig. 2C). Last, analysis of Δ190-196 $C1_{113}$ ^{13}Calpha chemical shifts yielded the position of the three alpha-helices within residues 147-159, 175-189 and 203-230, showing that the topology is conserved with respect to WT PrP (Fig. 2C).

The HTVTTTT deletion removed a histidine at position 190, which is the equivalent of His-187 in human PrP (Fig. S1). The pH-dependent protonation of this histidine is thought to play an important role in the electrostatic network and the stability of the globular part of PrP (25,26). But the deletion of the other residues might also impact the thermodynamic stability of the protein. We thus tested whether the deletion affected the stability using a thermal shift assay to determine the melting temperature of WT and mutant PrP. The melting temperature of Δ190-196 PrP (49.9°C) was reduced by 7°C compared to the WT PrP in sodium acetate buffer (10 mM, pH 5.0) (Fig 2D). A marked reduction of 8°C was also observed in these assays, using a different condition, sodium phosphate buffer (250 mM, pH 5.1), that increases the thermal stability of both WT and Δ190-196 recombinant PrPs (Fig. S2). Altogether these observations

indicate that Δ190-196 mutant PrP conserves the overall structure of WT PrP but loses some stability.

Expression of the mutant PrP^C in RK13 cells

Ovine Δ190-196 PrP was stably transfected in RK13 cells to generate sublines and clones referred to as Δ190-196 Rov. Mutant PrP was efficiently expressed as a glycoprotein in Rov cells. Western blotting showed that unglycosylated forms of Δ190-196 PrP^C were underrepresented compared to WT or Δ193-197 PrPs generated previously (23) (Fig. 3A). Deglycosylation by PNGase F treatment corroborated the high glycosylation level of Δ190-196 PrP and indicated that the mutant protein was smaller than WT PrP^C by about one kDa, as expected (Fig. 3B). Using an antibody with an epitope in the C-terminal part of PrP rather than in the N-terminal region allowed us to identify both the full-length protein and its natural C-terminal C1 fragment. PNGase treatment was required for accurate identification of PrP^C and C1, as they are both highly glycosylated. The relative proportion of the full-length PrP versus the C1 fragment was roughly similar for the WT and the mutant protein (Fig. 3C). Immunofluorescence showed colocalization of Δ190-196 PrP with WGA, a lectin marker of plasma membrane glycoconjugates, indicating that the mutant protein was correctly addressed to the Δ190-196 Rov cell surface (Fig. 3D) as with the WT protein (27,28). These observations indicate that Δ190-196 PrP has correct post-translational modifications and cell trafficking.

Spontaneous generation of a self-sustained protease-resistant form of PrP in Δ190-196 Rov

The expression of Δ190-196 PrP was turned on by addition of doxycycline and we followed the fate of the protein over cell passaging by Western blotting, checking for the appearance of PK-resistant forms. While Δ190-196 PrP was sensitive to PK digestion during the first passages, a PK-resistant form systematically appeared, usually after the 4^{th} or the 5^{th} passage (Fig. 4A). This protease-resistant form termed Δ190-196 PrP^{res} persisted for > 1 year of continuous culture (Fig. 5A). The electrophoretic profile of Δ190-196 PrP^{res} was characterized by a large smear of glycosylated species and presence of a well individualized faint band migrating at 14 kDa (Fig. 4A). A second weaker band migrating at 15.5-16 kDa was detected upon overexposure of the blots or when enough material was loaded on the gel (Fig. 5A). Treatment with PNGase F allowed resolving the whole emerging PK-resistant species in two major bands: a main 14 kDa species that had the same size than the C1 fragment and a larger less represented peptide above the 15 kDa molecular weight marker that will be further referred to as 16 kDa PrP^{res} (Fig. 4B). This indicated that the 14 kDa and 16 kDa bands identified without PNGase treatment (Figs. 4A and 5A) were non-glycosylated native forms of Δ190-196 PrP^{res}.

The spontaneous emergence of PK-resistant Δ190-196 PrP was reproducible and occurred systematically from bulk cultures of Δ190-196 Rov obtained from three independent transfections (Fig. 5B). Individual Δ190-196 Rov clones obtained by limiting dilution spontaneously produced Δ190-196 PrP^{res}, except for one clone, clone 12, despite expression of the mutant PrP to levels similar to those of other clones (Fig. 5C). This 'resistant' clone was useful for infection studies described in the following section and its existence suggested that currently unrecognized cellular factors are key for the spontaneous generation of Δ190-196 PrP^{res}. Δ190-196 Rov cells could be frozen and thawed, without affecting the generation of PK-resistant PrP species. This characteristic together with persistence in cell culture recalled that of prion infected cells.

We next examined whether the biochemical properties of Δ190-196 PrP^{Sc} resembled those of prions passaged in WT Rov cells. Δ190-196 Rov lysates were treated with increasing PK concentrations and analyzed by Western blotting. Δ190-196 PrP^{Sc} resisted to higher concentration of PK (Figs. 6A and 6B) than 127S prions propagated in WT Rov (Fig. 6C). Δ190-196 PrP^{res} was recovered by centrifugation at 20,000 x *g* after PK digestion indicating that it was insoluble and aggregated (Fig. 5A). The aggregation size of Δ190-196 PrP^{Sc} was determined by sedimentation velocity. Δ190-196 PrP^{Sc} formed assemblies with a size in the range of PrP^{Sc} assemblies formed by subfibrillar prions (Fig. 6D) according to previous reports (29,30). 127S PrP^{Sc} assemblies from Rov cells had slightly larger assemblies with respect to size (Fig. 6D). Whether the difference is due to the number of PrP-mers composing the assemblies or

to the density of their main core remains to be determined.
To summarize, introduction of the 190-196 deletion in RK13 cells favored the spontaneous and persistent production of PK-resistant PrP^{Sc} species with an atypical electrophoretic pattern. Δ190-196 PrP spontaneously adopted a conformation that showed hallmarks of a prion: insolubility, aggregation, protease resistance and cell perpetuation. We thus called this entity Δ^{Spont} prion.

Δ^{Spont} prion is infectious for cells expressing homologous or closely related mutant PrP

The infectious potential of Δ^{Spont} prions was primarily tested by cell-assay using Δ190-196 or WT Rov. As control, these cells were infected by 127S prions propagated in WT Rov. Naïve Δ190-196 Rov were susceptible to Δ190-196 lysates containing Δ^{Spont} as they produced PrP^{res} in large amount as soon as the second passage post-infection (Fig. 7), while mock-infected cells did not. In contrast, WT Rov were not infectible with Δ^{Spont} prions (Fig. 7). Conversely, 127S could propagate in WT Rov but not in Δ190-196 Rov, at least for the first passages, the spontaneous emergence of Δ^{Spont} prions on long-term passage obscuring the fate of 127S infection.
We next challenged the 'resistant' Δ190-196 cell clone 12 and found it readily susceptible to Δ^{Spont} prion infection. PrP^{res} was detected as soon as the second passage and up to passage 8 post-infection (Fig. 8A). Δ^{Spont} prions were thus *de novo* infectious for cells expressing the homologous mutant protein. The atypical profile of PrP^{res}, with the characteristic presence of 14 kDa and 16 kDa bands was faithfully conserved upon infection.
Previously, we established a set of Rov cells expressing PrP with deletions of different sizes in the C-terminus of helix H2. None of these cells produced spontaneously PK-resistant forms of mutant PrP (23). In particular, the Δ193-197 and Δ192-197 cells were susceptible to several ovine prions, including 127S. In contrast, the Δ190-197 cells were resistant to all of them (23). These three mutant cell lines were challenged with Δ^{spont} prions to determine whether Δ^{Spont} prion replication was strictly dependent on Δ190-196 PrP. Cells expressing PrP with 190-197, 192-197 or 193-197 deletions were all susceptible to Δ^{Spont} infection (Fig. 8A). The Δ^{Spont} PrP^{res} pattern was mostly maintained in the infected cells.
We knew from our previous work that 127S prions propagated on Δ193-197 Rov cells were still infectious for WT Rov cells, indicating a structural compatibility between this mutant and WT PrP for 127S prion conversion. It was thus appealing to determine whether Δ^{Spont} propagated on Δ193-197 Rov cells could similarly become infectious for WT cells. The results showed that this was not the case, although Δ^{Spont} prions propagated on Δ193-197 Rov cells were *de novo* infectious for naïve Δ193-197 cells (Fig. 8B). Similar results were obtained for Δ^{Spont} propagated on Δ192-197 Rov cells: it was *de novo* infectious for Δ192-197 Rov cells and infectious for Δ193-197 Rov cells but not for WT Rov cells (Fig. 8C).
Altogether, these cell-assays demonstrate the infectivity of Δ^{Spont} prions and their ability to propagate on cells expressing homologous Δ190-196 PrP or closely related mutants but not WT PrP. This suggests that a certain degree of compatibility in the H2 C-terminal sequence of PrP is required for conversion by Δ^{Spont} prions.

Molecular typing of Δ^{Spont} prions

Most prion strains can be grouped into two broad categories with respect to their molecular pattern, depending on the N-terminal endpoint of the C2 PrP^{res} fragment. Type 1 strains produce PrP^{res} species starting around position 85 of ovine PrP, while type 2 strains PrP^{res} species are shorter, beginning at position 100. The size of unglycosylated C2 PrP^{res} is thus a generic way to discriminate between strains. Therefore, we compared the electrophoretic profile of Δ^{Spont} PrP^{res} with 127S type 1 prion strain propagated on WT Rov cells and with type 1 ($T1^{Ov}$) and type 2 ($T2^{Ov}$) strain propagated on Δ193-196 Rov cells, which express a mutant PrP with a size closer to Δ190-196 PrP (Fig. 9). Based on the aglycosylated lower bands, we could ascertain that the main 14 kDa band of Δ^{spont} prion was shorter than any type 1 or type 2 C2 fragment and that the16 kDa PK-resistant band was just slightly shorter than the C2 fragment of the type 2 strain. The PrP^{res} electrophoretic profile of Δ^{spont} prions was thus clearly atypical with simultaneous presence of two major bands shorter than the usual PK-resistant C2 fragment from 'classical' prion strains.

To characterize in more details the nature of the 14 kDa and 16 kDa fragments from Δ^{Spont} PrP^{res}, we performed an epitope mapping with anti-PrP antibodies spanning the entire PrP C-terminus, after deglycosylation of PrP^{res} species. Signals produced by Sha31 and 8F9 mAbs were similar, indicating that Δ^{Spont} PrP^{res} species are C-terminal fragments of PrP (Fig. 10).

Regarding the major 14 kDa species, the band was not detected by 12B2 and 8G8 mAbs. Part of the 14 kDa band of higher molecular weight was recognized by 6C2 mAb and thus contained the full epitope of this antibody (114-HVAAAGA). The other part of lower molecular weight was 6C2 negative, indicating the loss of at least His-114 (Figs. 10 and S3). Therefore the 14 kDa band contained PrP^{res} polypeptides with different N-terminal endpoints at the vicinity of the main cleavage site reported for the C1 fragment (8,31). In non-infected WT Rov cells and in Δ^{Spont}-free Δ190-196 Rov cells (early passage), part of the C1-PrP^{C} fragment is 6C2-positive (Fig. S3), suggesting a certain variability in N-terminal endpoints. The PK-resistant 14 kDa band from Δ^{Spont} PrP^{res} could thus result either or both from protease-digestion of the misfolded full-length Δ190-196 PrP or from a conformational change of the C1 fragment.

Regarding the 16kDa band, the epitope mapping indicated a recognition by the 6C2 but not the 8G8 mAb. Therefore the N-terminus of these truncated PrP^{res} polypeptides starts between residues inside the 8G8 epitope (position 100 to 105) and residue 113 at the head of 6C2 epitope, most likely close to the 8G8 border based on the molecular weight of these fragments. A faint and fuzzy band was also observed just above the 16 kDa band with all the mAbs used. This indicated the presence of few Δ^{Spont} PrP^{res} species of larger size close to the C2 fragments from conventional prions.

Altogether these observations show that Δ190-196 PrP turned spontaneously into a misfolded form producing a complex pattern of PK-resistant species with a main core around 14 kDa. These PrP^{res} fragments of different size reflect the formation of different structures or assemblies by the misfolded protein. The prominence of the 14 kDa band raises the question of whether it could or not correspond to the minimum and necessary portion of Δ190-196 PrP for Δ^{Spont} replication as is the C2 fragment for classical prions. As a corollary this opens the unorthodox question of whether the mutant C1 fragment itself could misfold, either spontaneously or after conversion by Δ190-196 PrP^{Sc} species produced from the full-length mutant PrP.

Conversion of mutant C1 by Δ^{Spont} prions

To examine the possibility that mutant Δ190-196 C1 PrP^{C} (ΔC1) alone can misfold into PrP^{Sc}, either spontaneously or following infection by Δ^{Spont} prions, we generated Rov cells expressing solely Δ190-196 C1 PrP^{C}. The C1 fragment is generated by PrP^{C} cleavage at the alpha cleavage site, right upstream the N-terminal hydrophobic region. In human brain, the main C1 fragment starts at His-111 and was referred as to C1-upper but it can also start at Met-112 and was referred to as C1-lower (8). Varying degrees of proteolytically processed C1 fragments at equivalent positions were suggested for ovine PrP (31). We thus built two constructs to express the C1 part of ovine PrP flanked by the N and C-terminal signal peptides of ovine PrP. The WT and Δ190-196 $C1_{113}$ constructs were designed to start at residues Lys-113, one residue upstream His-114 the equivalent of His-111 in human PrP, to warrant both a correct and efficient cleavage of the N-terminal peptide signal and the presence of the full 6C2 epitope. The constructs referred as $C1_{115}$ were designed to start at Val-115 to produce an equivalent to the C1-lower fragment.

As with WT and Δ190-196 full-length PrP^{C}, the C1 fragments were highly glycosylated in RK13 cells (Fig. 11A), but the unglycosylated forms were expressed in lower proportion in the two Δ190-196 mutants than in the WT counterparts. The C1 proteins had the expected size (Fig. 11B) and were present at the cell surface (Fig. 11C and 11D), indicating that signal peptides were functional and processed by the cells.

In contrast to full length Δ190-196 PrP^{C}, mutant C1 PrP^{C} did not spontaneously convert into a PK-resistant form over passages, even after several months of cell culture (Fig. 12). However, upon exposure to Δ^{Spont} prions, these forms were converted into self-replicating PK-resistant PrP^{Sc} (Fig. 12). These PrP^{Sc} species were termed $\Delta C1^{Sc}$. C1 conversion process was specific to Δ^{Spont} prions and needed the Δ190-196 deletion. 127S prions were not able to convert WT or Δ190-196 C1 PrP^{C}. Δ^{Spont} prions were unable to convert WT C1 (Fig.

12), as it was previously unable to do so for full-length WT PrP (Fig. 7). As with WT PrP, a certain degree of sequence compatibility between the cellular substrate and the infecting prion is required for C1 conversion by Δ^{Spont} prion.

$\Delta C1^{Sc}$ are *de novo* infectious and preserve Δ^{Spont} PrP^{res} signature

We finally investigated the infectious potential of $\Delta C1_{113}{}^{Sc}$ and $\Delta C1_{115}{}^{Sc}$. We used, as inocula, cell lysates of Δ^{Spont}-infected Δ190-196 C1 at passage 8 (see above). Controls were made to exclude any remnant infectivity of Δ^{Spont} prions or spontaneous infectivity of the homogenates from cells expressing mutant C1 PrP^{C}. As shown in Figure 13, both $\Delta C1_{113}{}^{Sc}$ and $\Delta C1_{115}{}^{Sc}$ were *de novo* infectious for cells producing the homologous mutant ΔC1 proteins. In contrast cells expressing their WT counterparts were not susceptible to the infection. Remarkably, $\Delta C1^{Sc}$ exhibited the same activity as Δ190-196 PrP^{Sc} with respect to the panel of susceptible cells. PrP^{C} from 'resistant' Δ190-196 clone 12 and from the two closely related mutants Δ193-197 and Δ192-197 were converted into PK-resistant PrP^{Sc}. The western blot signature of PrP^{res} in these cells recalled that produced following Δ^{Spont} prion infection (compare Fig. 13 and Fig. 8A). Not only the characteristic 14 kDa band, but also the 16 kDa band were present, indicating additional conversion of the full-length proteins by $\Delta C1^{Sc}$. The main strain-specific determinant of Δ^{Spont} prions was thus enciphered in $\Delta C1_{113}{}^{Sc}$ or $\Delta C1_{115}{}^{Sc}$.

Discussion

This work focuses on the spontaneous, in-cell conversion of a deletion mutant PrP into a novel form of prion. Δ^{Spont} prions showed three main original features: an internal deletion of seven residues in the protease-resistant core, an unusual PrP^{res} signature and a remarkable capacity to propagate on the homologous C-terminal C1 segment of PrP, thus generating mutant C1 prions. In addition, this work provides a unique cell model to get insights in cell processes and factors associated with spontaneous prion emergence.

Spontaneous misfolding of ovine PrP with deletion in alpha-helix H2

Although spontaneous conversion of PrP into prion is a rare event, modifications in PrP can considerably increase this occurrence as not less than about forty disease-causing mutations are identified in inherited cases of human PrP (16). Spontaneous prion conversion also occurred in transgenic mice expressing some of these mutations (17-19,32,33). Conversion of equivalent mutant PrP in cell culture has so far been disappointing maybe in part because there is still no easy cell model for efficient human prion replication. We thus considered another approach that was to use a well-characterized reverse genetic model of prion replication and to remove from PrP highly conserved residues that might be important for PrP stability, while minimally affecting the overall structure. We previously identified the C-terminal region of the H2 alpha-helix as an area that meets these prerequisites. We found that the four contiguous threonine residues at the end of the helix were not necessary for replication of several ovine prion strains in RK13 cells (23). Deletion of the threonine cluster (Δ193-196) even favored the replication of strains difficult to propagate in cells expressing wild-type ovine PrP (23). Thus, we considered this deletion as a good starting point to facilitate the emergence and propagation of a spontaneous prion. As Δ193-196 deletion was insufficient to cause spontaneous conversion of mutant PrP, we extended it to the three upstream residues His-190, Thr-191 and Val-192. Similar residues in human PrP are associated with disease-causing mutations H187R, T188K and V189I responsible either for GSS or CJD (34-37), highlighting their potential importance for preservation of the normal form of the protein. We found that the simultaneous deletion of residues HTVTTTT maintained the overall PrP structure, but strongly reduced the stability of the recombinant ovine PrP. Reduced stability is expected to facilitate partial or complete unfolding of the protein and its spontaneous misfolding (38). Thus the Δ190-196 deletion might have introduced perturbations in the charge equilibrium, salt-bridges and/or hydrophobic interactions. His-187 in human PrP, equivalent to His-190 in ovine PrP, is thought to be a key residue of the electrostatic network stabilizing the globular helical domain of PrP (26,39). Protonation of histidine is pH-dependent and the positive charge acquired at acidic pH is thought to be involved in the

conformational shift of recombinant PrP *in vitro* (25,40,41). The disease-causing mutation H187R is one of the rare human mutations that markedly reduces PrP stability and this is attributed to replacement of histidine by a permanently positively charged residue (42). The deletion Δ190-196 not only removed His-190 residue but also brought Lys-197 in position 190, mimicking the replacement of His-190 by another permanently positively charged residue, recalling H187R mutation. This might have contributed to destabilization of Δ190-196 PrP and likely explains why the deletion Δ190-197, which eliminates the lysine residue did not lead to spontaneous prion generation, while the mutant protein remained convertible into PrP^{res} by Δ^{Spont} prions. In addition, replacement of each or all the four contiguous threonines (193-196) by different residues had also affected PrP stability (43,44). Any of these perturbations alone or in combination may have contributed to the spontaneous conversion of Δ190-196 PrP into Δ^{Spont} prions. The conservation of HTVTTTT sequence in mammalian PrPs might well reflect preservation of an important region for the dynamics and the maintenance of the helical folding of the protein in a cellular context.

Transmissibility of Δ^{Spont} prions

Δ190-196 PrP was sensitive to protease digestion. Yet after several cell passages, a PK-resistant form systematically emerged, indicating spontaneous conformational change of the mutant PrP. The spontaneous formation of PK-resistant PrP was verified in one occasion by an experiment of cell transfection and culture entirely carried out in prion free laboratory, excluding inadvertent contamination. The Δ190-196, or Δ^{Spont} PrP^{Sc} entity as we called it, was shown to be a self-propagating, protease-resistant, insoluble and aggregated form that was transmissible to other cells. Δ^{Spont} thus showed all the usual hallmarks of prion replication in cell culture. A basic characteristic of prions is their ability to transmit their own conformational state to homologous PrP^{C} and in some instance to heterologous PrP^{C}. Persistence of Δ190-196 PrP^{Sc} in cell culture indicated some replication but as we faced a spontaneous conversion that might be reiterated at each passage, we demonstrated *de novo* infectivity of Δ^{Spont} prion in several cell-assays: i- earlier accumulation of Δ190-196 PrP^{Sc} in exposed cells; ii- infection of the Δ190-196 Rov clone 12 that did not produce spontaneously a PK-resistant form of the mutant protein; iii- infection of Rov cells expressing the Δ190-196 C1 PrP^{C}; and iv- infection of Rov cells expressing three other mutant PrPs with close deletions in H2 C-terminus, notably the Δ190-197 mutant that was refractory to infection by conventional ovine prion strains (23). Sequence proximity and/or structural adaptability between Δ^{Spont} and Δ190-197 PrP might explain it. In contrast, conversion of WT PrP by Δ^{Spont} prions failed despite many attempts and the use of different cell populations including the historic Rov clone 9 (27) or more susceptible clones (45). In a previous work, we found that the 127S ovine prion strain propagated on WT PrP was easily propagated on Δ193-197 Rov cells and reciprocally (23), suggesting a good structural compatibility for conversion between the Δ193-197 mutant and WT PrP when this strain is concerned. Here, Δ^{Spont} prion propagated on Δ193-197 PrP was still not able to convert WT PrP, indicating that the Δ193-197 PrP^{Sc} structure transmitted by Δ^{Spont} prion rather than only sequence of the mutant protein causes the transmission barrier.

Biochemical specificities of Δ^{Spont} PrP^{Sc}

The PrP^{res} pattern of Δ^{Spont} was faithfully maintained in the different cell assays. The pattern was complex and showed differentially represented bands corresponding to N-terminal truncations at different end points. It did not fit with any known prion strains regarding the 14 kDa and 16 kDa bands. The minor 16 kDa band was slightly more N-terminally truncated than the classic C2 fragment from type 2 prions. The major 14 kDa band had a size close or similar to that of the C1 fragment of Δ190-196 PrP. These two bands were found in individual clones of Δ190-196 Rov cells with similar relative proportion as in populations of transfected cells. A third, minor, 8G8/12B2 positive band was identified that might be close or similar to that of more classical type1 prions. Thus Δ^{Spont} PrP^{res} included fragments close to C2 of type 1 and type 2 plus prominent C1-like species. C2-like protease-resistant fragments are most probably truncated forms of full-length mutant Δ190-196 PrP^{Sc}, while C1-like PrP^{res} species might result from conversion of either or both the full-length mutant PrP and its C1 fragment. The unconventional PrP^{res}

profile of Δ^{Spont} prion strongly suggests an original structural organization but might be complicated by conversion of two substrates, the full-length protein and its C1 fragment, rather than only full-length PrP for more classical prions.

Generation of Δ190-196 C1 prion

PrP^{C} is naturally cleaved into a C-terminal C1 fragment and its complementary N-terminal N1 at the alpha cleavage site. This cleavage, the efficacy of which is cell-dependent, was attributed to metalloproteases of the ADAM family, but the exact nature of the enzyme remains a subject of controversy and may depend on tissues or cell lines considered (46-50). Moreover, the cleavage is not dependent on a specific sequence and whether it occurs at the cell surface or inside the cell between the Golgi and the plasma membrane is not clearly established (51,52). In Rov cells, the C1 fragment appears as a relatively large N-terminally truncated band, beginning around position His-114 or Val-115 equivalent to that determined in human brain (8,31). A consensus is that the C1 fragment of PrP^{C} is shorter than the PrP^{res} domain and thus cannot be converted into prion. Furthermore, an apparent inverse correlation between C1 levels and cell susceptibility to prions was reported in cell lines as well as a dominant negative effect on prion replication in transgenic mice overexpressing C1 (14,53). Thus, the C1 fragment is often considered as a competitive inhibitor of PrP^{C} conversion. We found here different outcomes. The main PrP^{res} domain of Δ^{Spont} prions had a size close or similar to that of C1, and Δ^{Spont} prions were able to convert the mutant form of C1. Protease resistant $\Delta C1^{Sc}$ showed hallmarks of prion replication in cell culture and was transmissible *de novo* to cells expressing either the homologous C1 protein, the homologous full-length mutant PrP or closely related mutants. To the best of our knowledge there is no other report of confirmed conversion of C1 or C1-like polypeptides. Two presumptive bovine spongiform encephalopathy cases with C1-like PrP^{res} signature were reported but they were finally found to lack prion infectivity after inoculation of brain material to cattle and to bovine PrP transgenic mice (54,55). The exceptional conversion of ΔC1 into prion after infection by the unconventional Δ^{Spont} prion is likely due to the conjunction of the sequence modification introduced in the polypeptide and adoption of a misfolded structure significantly different from that of the other prions.

$\Delta C1^{Sc}$ as a driving force for the propagation of the Δ^{Spont} prion

ΔC1 prions had templating activity on the full-length mutant proteins and preserved the PrP^{res} signature of Δ^{Spont} prion. Indeed, infection by ΔC1 prions produced not only C1-like PrP^{res} but also C2-like 16 kDa species that were larger than C1 and thus resulted from conversion of the full-length protein. $\Delta C1^{Sc}$ therefore behaves like a prion strain which maintains the structural information associated with the specific biochemical profile of Δ^{Spont} prion. This strongly suggests that the 14 kDa ΔC1-like PrP^{res} core produced by spontaneous conversion of Δ190-196 PrP has at least contributed to Δ^{Spont} prion propagation and might even be the most important template for the normally folded mutant protein.

As ΔC1 did not spontaneously form a prion, the primary event in Δ^{Spont} prion formation may be the spontaneous conversion of full-length PrP. Then the reciprocal capacity of Δ190-196 PrP^{Sc} to induce conversion of ΔC1 fragment and of $\Delta C1^{Sc}$ to induce full-length mutant PrP conversion would lead to Δ^{Spont} complex pattern.

It was unexpected that the short $\Delta C1_{115}$ or $\Delta C1_{113}$ fragments, with lengths of 113 and 115 residues, respectively could be sufficient to adopt a specific transmissible prion structure, as the lack of WT C1 convertibility into prion was explained by its shortened size compared to C2 PrP^{res} fragments. Whether ΔC1 prion adopts a structure close to C2 but without the 15 or 30 N-terminal residues or a different structural organization remains an unresolved question. Δ^{Spont} and even more ΔC1 prions recall somehow PrP106, a mouse PrP with a double deletion (Δ23–88, Δ141–176), that produced a miniprion following infection by RML strain, but not spontaneously (56). The sequence of this mutant protein was very different from that of Δ190-196 ovine PrP or C1. The sequence of PrP106 contained about 20 residues upstream of the mouse C1 segment and a large internal deletion that removed both H1, the beta2 strand and five N-terminal residues of H2 (56), together with the loops between H1 and H2 that are considered to be highly important for prion conversion (57-59). While structurally different from ΔC1 prion, the miniprion is another example of prion entity

constituted from elements of the PrP sequence. A third more distant example of short PrP sequence associated with prion formation is the human PrP with Y145-Stop mutation associated with GSS (60). In contrast to the two precedent mutants, PrP Y145-Stop conserves only the N-terminal moiety of PrP and lacks the whole globular helical domain. Δ^{Spont} and Δ190-196 C1 prions generated in this work are therefore original and attractive prion entities which deserve to be studied further with transgenic mouse models in the future.

Conclusion

We report the generation of a novel spontaneous mutant prion propagating in cell culture and conversion into prion of both the full-length and the C-terminal C1 fragment of Δ190-196 mutant PrP. We demonstrated that only 113 or 115 residues of the PrP C-terminus are sufficient to constitute a self-replicating and transmissible prion entity. Our results also suggest also that the HTVTTTT conserved sequence in the H2 C-terminus of PrP is important for prion protein stability and that removal of H2 C-terminal residues is required for productive infection in cells challenged by the spontaneous prion. This work also provides a unique cell culture model for spontaneous prion formation to further study cell factors and molecular processes involved.

Experimental procedures

Plasmid constructs

Sheep Prnp ORF encoding PrP allotype VRQ (Val-136, Arg-154, Gln-171) was cloned into pTRE plasmid of the pTeT-on expression system (Clontech) (27). Deletions of residues HTVTTTT (position 190 to 196) and N-terminal deletions Δ25-112 and Δ25-114 to generate wild-type and mutant versions of $C1_{113}$ and $C1_{115}$ were performed by site-directed mutagenesis (QuikChange II mutagenesis kit; Stratagene). Each mutant construct was verified by sequencing.

Antibodies

The anti-PrP monoclonal antibodies (mAbs) used were as follows: 4F2 directed to the octa-repeat domain (residues 62 to 94 according to sheep PrP numbering) (61,62), 12B2 (residues 93-97) (63), 8G8 (residues 100-105) (61,62), 6C2 (residues 114-121) (64) (Central Veterinary Institute, Wageningen UR, Netherland) Sha31 (residues 148-155) (62) (Bertin Pharma), and 8F9 (residues 224-234) (65). Sha31and 8G8 were biotinylated and further detected with horseradish peroxidase-conjugated streptavidin. For other mAbs, secondary antibodies were peroxidase-conjugated goat anti-mouse IgG (Abliance) used at 1:5000.

Cell culture and isolation of Rov cells

Rov cells are epithelial RK13 cells that stably express either wild-type or mutant ovine PrP in an inducible manner, by using a tetracycline-inducible system (27). They were obtained by transfection of cells by lipofectamine and puromycin selection. We used cell populations produced by a pool of puromycin-resistant cells, unless indicated otherwise. In some occasions, we used individual clones that were obtained by serial dilution of transfected cells in presence of the selecting agent. Cells were grown in Opti-MEM medium (Invitrogen) supplemented with 10% fetal calf serum (FCS) and antibiotics, and split at 1:4 after trypsin dissociation once a week. To express full-length PrP^{C} or C-terminal C1 polypeptides, cells were cultivated in the continuous presence of 1μg/ml of doxycycline (Sigma).

Prions and prion strains

The spontaneous mutant prion Δ^{Spont} was propagated on Rov cells expressing the Δ190-196 PrP mutant unless stated otherwise. The 127S ovine prion strain was isolated through serial transmission and cloning by limiting dilution of PG127 field scrapie isolate to tg338 transgenic mice expressing the VRQ allele of ovine PrP (66,67). 127S was propagated on Rov cells expressing the WT PrP for comparative infection test or determination of PrP^{res} profile. $T1^{Ov}$ and $T2^{Ov}$ prions were originally isolated from serial transmission of a human sporadic CJD case (MM2 type) to tg338 mice (45). For comparison of PrP^{res} profiles with Δ^{Spont}, $T1^{Ov}$

and $T2^{Ov}$ strains were previously propagated on Rov cells expressing Δ193-196 mutant PrP (23).

Prion infection of cell cultures

To test the infectivity of cell cultures, cells were pelleted, frozen and thawed three times, sonicated three times for 30 seconds and the resulting homogenates were used as inocula to infect naive cell cultures as previously described (23,68). Homogenates were left three days on the challenged cells. They were then washed with PBS, trypsinized and seeded at 1/10 dilution in fresh culture medium. Cells were then split at 1:4 dilution after one week of culture as for each other successive passage. For infection by Δ^{Spont} prion, homogenates of Δ190-196 Rov cells harvested at least 9 passages after the addition of doxycycline were used. To test for infectivity of Δ^{Spont} propagated on Rov cells expressing other deletion mutant PrP or C-terminal C1 polypeptides, inocula were made from cells harvested 8 passages post exposure.

Cell lysis, protease digestion, and PNGase F treatment

Cells were washed twice with cold phosphate-buffered saline and whole-cell lysates were prepared in TL1 buffer (50 mM Tris-HCl [pH 7.4], 0.5% sodium deoxycholate, 0.5% Triton X-100). Lysates were clarified by centrifugation for 2 min at 800g, and protein concentrations were determined by microBCA assay (Pierce). For PrP^{res}, lysates were incubated with 8µg of PK per 1 mg of protein for 2 h at 37°C and then centrifuged for 30 min at 22,000 x g. Pellets were dissolved in Laemmli sample buffer and boiled for 15 min at 100°C. When needed, 500 U of PNGase F (New England BioLabs, Massachusetts) and 1% Nonidet P-40 were added to denatured proteins that were further incubated at 37°C overnight.

Sedimentation velocity fractionation

Experiments were performed as previously described (30). Briefly, cells were solubilized by addition of a buffer containing 4% (w/v) dodecyl-β-D maltoside and benzonase (0.4 unit/µl). After incubation for 30 min at 37°C, sarkosyl (N-lauryl sarcosine) was added to give a final concentration of 2% (w/v) in the samples. The incubation was pursued for 30 min at 37°C. 150 µl of solubilized samples were carefully loaded on a 4.8 ml continuous 10–25% iodixanol gradient (Optiprep, Sigma-Aldrich), with a final concentration of 25 mM HEPES pH 7.4, 150 mM NaCl, 2 mM EDTA, 0.5% Sarkosyl. The gradients were centrifuged at 285 000 g at 4°C for 45 min in a swinging-bucket SW-55 rotor. 30 fractions of 160µL were collected and PK-treated at a final concentration of 50 µg/ml for 1 hour at 37°C. PrP^{res} contents were analyzed by Western blotting using a biotinylated anti-PrP Sha31 monoclonal antibody. Signal intensities were quantified using ImageLab software (Bio Rad) and converted into arbitrary units after normalization. A fixed quantity of human recombinant PrP was employed to calibrate the PrP signals in different gels.

Immunoblotting and detection of PrP^{C} and PrP^{res}

Either 4 to 12% NuPage Bis-Tris precast polyacrylamide gels (Invitrogen) or 12% Criterion XT Bis-Tris gels (Bio- Rad) were used for sodium dodecyl sulfate polyacrylamide gel electrophoresis. For PrP^{C} analysis, 50 µg of protein per sample was loaded on the gel. For PrP^{res}, unless otherwise indicated, the samples corresponding to PK-resistant PrP contained in 25 or 50 µg of cell lysate protein were loaded onto the gel. The transfer of proteins, their detection, and their revelation were described previously (28,69).

Immunofluorescence, image acquisition and treatment

Cells were grown on plastic dishes or on glass coverslips in regular medium, washed twice with PBS before fixation for 10 minutes with 4% paraformaldehyde. Cells were then washed and incubated with the required monoclonal primary antibody (4F2 or Sha31, at 1:5000) in a blocking reagent buffer containing 0.5 % crystallin (Roche diagnostic) and 0.1% Tween 20 in PBS. After washing, cells were incubated with secondary Alexa Fluor 488-conjugated anti-mouse IgG antibodies (Molecular probes, Invitrogen) used at a

1:500 dilution, as previously reported (28,70) and nuclei were stained with 4',6-diamidino-2-phenylindole (DAPI). To specifically label the cell surface, Rhodamine-conjugated wheat germ agglutinin (WGA, Invitrogen) was incubated for 5 minutes with living cells, washed once with PBS and cells were further fixed and processed as described above. Images were acquired either with an Axio observer Z1 microscope (Zeiss) equipped with a CoolSnap HQ2 camera (Photometrics) and driven by the Axio-vision imaging system software. For some experiments, confocal microscopy was performed with a Zeiss LSM 700 microscope (MIMA2 Platform, INRA Jouy-en-Josas, France, http://www6.jouy.inrae/mima2) using a Plan-Neofluar x40 (NA 1.3) or Plan-Apochromat ×63 (NA 1.4) oil-immersion objective. Images were analyzed using the ImageJ 1.49v software (Wayne Rasband, NIH, USA, http://rsb.info.nih.gov/ij/).

Expression and purification of recombinant PrP

Recombinant proteins were produced and purified from *Escherichia coli* as published previously (23). Briefly, by site-directed mutagenesis the deletion Δ190-196 was introduced inside the sequence of the full-length ovine PrP (residues 25 to 234, VRQ allele) cloned into a pET28 expression vector. Wild-type and mutant proteins produced by *E. coli* were purified by immobilized metal affinity chromatography (IMAC) on Nickel columns.

Circular dichroism

The secondary structure of recombinant PrP produced by *E. coli* was analyzed by circular dichroism (CD). Measurements were carried out on Jasco-810 spectropolarimeter. Far-UV CD spectra of full length ovine PrP and the deletion mutant 190-196 were recorded from 260 to 180 nm at 25ºC in 1 µm path-length quartz cuvette at a protein concentration of 50 µM in 10 mM Na-acetate buffer at pH 5.0. Each CD spectrum was obtained by averaging 6 scans collected at a scan rate of 200 nm/min. Baseline spectra obtained with buffer were subtracted for all spectra.

Nuclear Magnetic Resonance

2D ^{1}H-^{15}N HSQC and 3D HNCA spectra of 250 µM recombinant ^{15}N^{13}C-labeled Δ190-196 $C1_{113}$ in 10 mM Na acetate pH 5 buffer were acquired on a Bruker NMR AVANCE III spectrometer equipped with a cryoprobe at a magnetic field of 18.8 T and a temperature of 298 K. ^{13}Calpha chemical shifts were analyzed by TALOS-N software by excluding similar sequences (71)

Fluorescence-based thermal shift assay

Reaction mixtures containing 10 or 20 µM of recombinant PrP in 10 mM Na acetate pH 5.0 and SYPRO orange (diluted 500-fold from a 5000-fold stock solution; Invitrogen), were made in duplicate in a 96-well fast PCR plate at a final volume of 20 µL. The experiments were also reproduced in buffer 250 mM Na Phosphate pH 5.1 (supporting information Fig. S2). The temperature gradient was carried out in the range of 10 °C to 95 °C, at 3 °C/min with a StepOnePlus real-time PCR system (Applied Biosystems) as previously described (72). Fluorescence was recorded as a function of temperature in real time (excitation with a blue LED source and emission filtered through a 5-carboxy-X-rhodamine [ROX] emission filter). The melting temperature (Tm) was calculated with the StepOne software v1.3 (Applied Biosystems) as the maximum of the derivative of the resulting SYPRO Orange fluorescence curves.

Data availability

All data in this study are contained within the manuscript.

Acknowledgments
We are grateful to the Microscopy and Imaging Facility for Microbes, Animals and Foods platform at INRAE (http://www6.jouy.inrae/mima2) and specially to Pierre Adenot for confocal facilities. We are grateful for Ile-de-France region (DIM 1Health) and the French Fondation pour la Recherche Médicale for their support and DL acknowledges ED ABIES of Paris-Saclay University for doctoral training.

Funding and additional information
This work was primarily supported by the Fondation pour la Recherche Médicale (FRM) (FRM team funding no. DEQ20150331689) and by the Conseil Regional, Ile-de-France (Ile-de- France Regional Council) (DIM 1Health). CMM was supported by postdoctoral fellowships from CONICYT-Becas Chile and DEFRA (United Kingdom) and DL by doctoral fellowship of Ile-de-France region (DIM 1Health). Master traineeships of CB were supported by l'Ecole Pratique des Hautes Etudes (EPHE).

Author contributions. C. M. M., D. L., and M. D. cell cultures, infection experiments and analysis; C. M. M., design and generation of the mutant PrP plasmids and cells; D. L., and C. S. NMR experiments and analysis; C. B., and M. D. design and production of WT and mutant C1 plasmids and cells; A. E. performed velocity sedimentation experiments and analysis; S. T. confocal analysis; E. J., and N. N. thermal stability assays; M. M. researched data; M. D. conceptualization, work supervision, writing preliminary version of the manuscript; V. B., writing and editing; C. S., writing NMR results and conclusions; V. B. and H. R. funding and team management; all the authors have read and improved the manuscript.

Conflict of interest
The authors declare no conflicts of interest in regards to this manuscript

References

1. Prusiner, S. B. (2013) Biology and genetics of prions causing neurodegeneration. *Annu Rev Genet* **47**, 601-623
2. Zahn, R., Liu, A., Luhrs, T., Riek, R., von Schroetter, C., Lopez Garcia, F., Billeter, M., Calzolai, L., Wider, G., and Wuthrich, K. (2000) NMR solution structure of the human prion protein. *Proc Natl Acad Sci U S A* **97**, 145-150
3. Prusiner, S. B. (1982) Novel proteinaceous infectious particles cause scrapie. *Science* **216**, 136-144
4. Come, J. H., Fraser, P. E., and Lansbury, P. T., Jr. (1993) A kinetic model for amyloid formation in the prion diseases: importance of seeding. *Proc Natl Acad Sci U S A* **90**, 5959-5963
5. Groveman, B. R., Dolan, M. A., Taubner, L. M., Kraus, A., Wickner, R. B., and Caughey, B. (2014) Parallel in-register intermolecular beta-sheet architectures for prion-seeded prion protein (PrP) amyloids. *J Biol Chem* **289**, 24129-24142
6. Spagnolli, G., Rigoli, M., Orioli, S., Sevillano, A. M., Faccioli, P., Wille, H., Biasini, E., and Requena, J. R. (2019) Full atomistic model of prion structure and conversion. *PLoS Pathog* **15**, e1007864
7. Baskakov, I. V., Caughey, B., Requena, J. R., Sevillano, A. M., Surewicz, W. K., and Wille, H. (2019) The prion 2018 round tables (I): the structure of PrP(Sc). *Prion* **13**, 46-52
8. Chen, S. G., Teplow, D. B., Parchi, P., Teller, J. K., Gambetti, P., and Autilio-Gambetti, L. (1995) Truncated forms of the human prion protein in normal brain and in prion diseases. *J Biol Chem* **270**, 19173-19180

9. Fischer, M., Rulicke, T., Raeber, A., Sailer, A., Moser, M., Oesch, B., Brandner, S., Aguzzi, A., and Weissmann, C. (1996) Prion protein (PrP) with amino-proximal deletions restoring susceptibility of PrP knockout mice to scrapie. *EMBO J* **15**, 1255-1264
10. Rossi, M., Baiardi, S., and Parchi, P. (2019) Understanding Prion Strains: Evidence from Studies of the Disease Forms Affecting Humans. *Viruses* **11**
11. Dickinson, A. G., Meikle, V. M., and Fraser, H. (1968) Identification of a gene which controls the incubation period of some strains of scrapie agent in mice. *J Comp Pathol* **78**, 293-299
12. Mange, A., Beranger, F., Peoc'h, K., Onodera, T., Frobert, Y., and Lehmann, S. (2004) Alpha- and beta- cleavages of the amino-terminus of the cellular prion protein. *Biol Cell* **96**, 125-132
13. Shmerling, D., Hegyi, I., Fischer, M., Blattler, T., Brandner, S., Gotz, J., Rulicke, T., Flechsig, E., Cozzio, A., von Mering, C., Hangartner, C., Aguzzi, A., and Weissmann, C. (1998) Expression of amino-terminally truncated PrP in the mouse leading to ataxia and specific cerebellar lesions. *Cell* **93**, 203-214
14. Westergard, L., Turnbaugh, J. A., and Harris, D. A. (2011) A naturally occurring C-terminal fragment of the prion protein (PrP) delays disease and acts as a dominant-negative inhibitor of PrPSc formation. *J Biol Chem* **286**, 44234-44242
15. Cobb, N. J., and Surewicz, W. K. (2009) Prion diseases and their biochemical mechanisms. *Biochemistry* **48**, 2574-2585
16. Mead, S., Lloyd, S., and Collinge, J. (2019) Genetic Factors in Mammalian Prion Diseases. *Annu Rev Genet* **53**, 117-147
17. Jackson, W. S., Borkowski, A. W., Watson, N. E., King, O. D., Faas, H., Jasanoff, A., and Lindquist, S. (2013) Profoundly different prion diseases in knock-in mice carrying single PrP codon substitutions associated with human diseases. *Proc Natl Acad Sci U S A* **110**, 14759-14764
18. Friedman-Levi, Y., Meiner, Z., Canello, T., Frid, K., Kovacs, G. G., Budka, H., Avrahami, D., and Gabizon, R. (2011) Fatal prion disease in a mouse model of genetic E200K Creutzfeldt-Jakob disease. *PLoS Pathog* **7**, e1002350
19. Watts, J. C., and Prusiner, S. B. (2017) Experimental Models of Inherited PrP Prion Diseases. *Cold Spring Harb Perspect Med* **7**
20. Stohr, J., Watts, J. C., Legname, G., Oehler, A., Lemus, A., Nguyen, H. O., Sussman, J., Wille, H., DeArmond, S. J., Prusiner, S. B., and Giles, K. (2011) Spontaneous generation of anchorless prions in transgenic mice. *Proc Natl Acad Sci U S A* **108**, 21223-21228
21. Watts, J. C., Giles, K., Bourkas, M. E., Patel, S., Oehler, A., Gavidia, M., Bhardwaj, S., Lee, J., and Prusiner, S. B. (2016) Towards authentic transgenic mouse models of heritable PrP prion diseases. *Acta Neuropathol* **132**, 593-610
22. Dima, R. I., and Thirumalai, D. (2004) Probing the instabilities in the dynamics of helical fragments from mouse PrPC. *Proc Natl Acad Sci U S A* **101**, 15335-15340
23. Munoz-Montesino, C., Sizun, C., Moudjou, M., Herzog, L., Reine, F., Chapuis, J., Ciric, D., Igel-Egalon, A., Laude, H., Beringue, V., Rezaei, H., and Dron, M. (2016) Generating Bona Fide Mammalian Prions with Internal Deletions. *J Virol* **90**, 6963-6975
24. Munoz-Montesino, C., Sizun, C., Moudjou, M., Herzog, L., Reine, F., Igel-Egalon, A., Barbereau, C., Chapuis, J., Ciric, D., Laude, H., Beringue, V., Rezaei, H., and Dron, M. (2017) A stretch of residues within the protease-resistant core is not necessary for prion structure and infectivity. *Prion* **11**, 25-30
25. Bae, S. H., Legname, G., Serban, A., Prusiner, S. B., Wright, P. E., and Dyson, H. J. (2009) Prion proteins with pathogenic and protective mutations show similar structure and dynamics. *Biochemistry* **48**, 8120-8128
26. Lee, J., and Chang, I. (2019) Structural insight into conformational change in prion protein by breakage of electrostatic network around H187 due to its protonation. *Sci Rep* **9**, 19305
27. Vilette, D., Andreoletti, O., Archer, F., Madelaine, M. F., Vilotte, J. L., Lehmann, S., and Laude, H. (2001) Ex vivo propagation of infectious sheep scrapie agent in heterologous epithelial cells expressing ovine prion protein. *Proc Natl Acad Sci U S A* **98**, 4055-4059

28. Salamat, M. K., Dron, M., Chapuis, J., Langevin, C., and Laude, H. (2011) Prion propagation in cells expressing PrP glycosylation mutants. *J Virol* **85**, 3077-3085
29. Tixador, P., Herzog, L., Reine, F., Jaumain, E., Chapuis, J., Le Dur, A., Laude, H., and Beringue, V. (2010) The physical relationship between infectivity and prion protein aggregates is strain-dependent. *PLoS Pathog* **6**, e1000859
30. Igel-Egalon, A., Moudjou, M., Martin, D., Busley, A., Knapple, T., Herzog, L., Reine, F., Lepejova, N., Richard, C. A., Beringue, V., and Rezaei, H. (2017) Reversible unfolding of infectious prion assemblies reveals the existence of an oligomeric elementary brick. *PLoS Pathog* **13**, e1006557
31. Tveit, H., Lund, C., Olsen, C. M., Ersdal, C., Prydz, K., Harbitz, I., and Tranulis, M. A. (2005) Proteolytic processing of the ovine prion protein in cell cultures. *Biochem Biophys Res Commun* **337**, 232-240
32. Jackson, W. S., Borkowski, A. W., Faas, H., Steele, A. D., King, O. D., Watson, N., Jasanoff, A., and Lindquist, S. (2009) Spontaneous generation of prion infectivity in fatal familial insomnia knockin mice. *Neuron* **63**, 438-450
33. Mercer, R. C. C., Daude, N., Dorosh, L., Fu, Z. L., Mays, C. E., Gapeshina, H., Wohlgemuth, S. L., Acevedo-Morantes, C. Y., Yang, J., Cashman, N. R., Coulthart, M. B., Pearson, D. M., Joseph, J. T., Wille, H., Safar, J. G., Jansen, G. H., Stepanova, M., Sykes, B. D., and Westaway, D. (2018) A novel Gerstmann-Straussler-Scheinker disease mutation defines a precursor for amyloidogenic 8 kDa PrP fragments and reveals N-terminal structural changes shared by other GSS alleles. *PLoS Pathog* **14**, e1006826
34. Colucci, M., Moleres, F. J., Xie, Z. L., Ray-Chaudhury, A., Gutti, S., Butefisch, C. M., Cervenakova, L., Wang, W., Goldfarb, L. G., Kong, Q., Ghetti, B., Chen, S. G., and Gambetti, P. (2006) Gerstmann-Straussler-Scheinker: a new phenotype with 'curly' PrP deposits. *J Neuropathol Exp Neurol* **65**, 642-651
35. Finckh, U., Muller-Thomsen, T., Mann, U., Eggers, C., Marksteiner, J., Meins, W., Binetti, G., Alberici, A., Sonderegger, P., Hock, C., Nitsch, R. M., and Gal, A. (2000) High frequency of mutations in four different disease genes in early-onset dementia. *Ann N Y Acad Sci* **920**, 100-106
36. Di Fede, G., Catania, M., Atzori, C., Moda, F., Pasquali, C., Indaco, A., Grisoli, M., Zuffi, M., Guaita, M. C., Testi, R., Taraglio, S., Sessa, M., Gusmaroli, G., Spinelli, M., Salzano, G., Legname, G., Tarletti, R., Godi, L., Pocchiari, M., Tagliavini, F., Imperiale, D., and Giaccone, G. (2019) Clinical and neuropathological phenotype associated with the novel V189I mutation in the prion protein gene. *Acta Neuropathol Commun* **7**, 1
37. Kotta, K., Paspaltsis, I., Bostantjopoulou, S., Latsoudis, H., Plaitakis, A., Kazis, D., Collinge, J., and Sklaviadis, T. (2006) Novel mutation of the PRNP gene of a clinical CJD case. *BMC Infect Dis* **6**, 169
38. van der Kamp, M. W., and Daggett, V. (2010) Pathogenic mutations in the hydrophobic core of the human prion protein can promote structural instability and misfolding. *J Mol Biol* **404**, 732-748
39. Xu, Z., Liu, H., Wang, S., Zhang, Q., Yao, X., Zhou, S., and Liu, H. (2020) Unraveling the Molecular Mechanism of Prion H2 C-Terminus Misfolding by Metadynamics Simulations. *ACS Chem Neurosci* **11**, 772-782
40. Hadzi, S., Ondracka, A., Jerala, R., and Hafner-Bratkovic, I. (2015) Pathological mutations H187R and E196K facilitate subdomain separation and prion protein conversion by destabilization of the native structure. *FASEB J* **29**, 882-893
41. Hosszu, L. L., Tattum, M. H., Jones, S., Trevitt, C. R., Wells, M. A., Waltho, J. P., Collinge, J., Jackson, G. S., and Clarke, A. R. (2010) The H187R mutation of the human prion protein induces conversion of recombinant prion protein to the PrP(Sc)-like form. *Biochemistry* **49**, 8729-8738
42. Malevanets, A., Chong, P. A., Hansen, D. F., Rizk, P., Sun, Y., Lin, H., Muhandiram, R., Chakrabartty, A., Kay, L. E., Forman-Kay, J. D., and Wodak, S. J. (2017) Interplay of buried histidine protonation and protein stability in prion misfolding. *Sci Rep* **7**, 882

43. Singh, J., Kumar, H., Sabareesan, A. T., and Udgaonkar, J. B. (2014) Rational stabilization of helix 2 of the prion protein prevents its misfolding and oligomerization. *J Am Chem Soc* **136**, 16704-16707
44. Abskharon, R., Wang, F., Vander Stel, K. J., Sinniah, K., and Ma, J. (2016) The role of the unusual threonine string in the conversion of prion protein. *Sci Rep* **6**, 38877
45. Chapuis, J., Moudjou, M., Reine, F., Herzog, L., Jaumain, E., Chapuis, C., Quadrio, I., Boulliat, J., Perret-Liaudet, A., Dron, M., Laude, H., Rezaei, H., and Beringue, V. (2016) Emergence of two prion subtypes in ovine PrP transgenic mice infected with human MM2-cortical Creutzfeldt-Jakob disease prions. *Acta Neuropathol Commun* **4**, 10
46. Corda, E., Du, X., Shim, S. Y., Klein, A. N., Siltberg-Liberles, J., and Gilch, S. (2018) Interaction of Peptide Aptamers with Prion Protein Central Domain Promotes alpha-Cleavage of PrP(C). *Mol Neurobiol* **55**, 7758-7774
47. Vincent, B., Paitel, E., Saftig, P., Frobert, Y., Hartmann, D., De Strooper, B., Grassi, J., Lopez-Perez, E., and Checler, F. (2001) The disintegrins ADAM10 and TACE contribute to the constitutive and phorbol ester-regulated normal cleavage of the cellular prion protein. *J Biol Chem* **276**, 37743-37746
48. Altmeppen, H. C., Prox, J., Puig, B., Kluth, M. A., Bernreuther, C., Thurm, D., Jorissen, E., Petrowitz, B., Bartsch, U., De Strooper, B., Saftig, P., and Glatzel, M. (2011) Lack of a-disintegrin-and-metalloproteinase ADAM10 leads to intracellular accumulation and loss of shedding of the cellular prion protein in vivo. *Mol Neurodegener* **6**, 36
49. Liang, J., Wang, W., Sorensen, D., Medina, S., Ilchenko, S., Kiselar, J., Surewicz, W. K., Booth, S. A., and Kong, Q. (2012) Cellular prion protein regulates its own alpha-cleavage through ADAM8 in skeletal muscle. *J Biol Chem* **287**, 16510-16520
50. Wik, L., Klingeborn, M., Willander, H., and Linne, T. (2012) Separate mechanisms act concurrently to shed and release the prion protein from the cell. *Prion* **6**, 498-509
51. Walmsley, A. R., Watt, N. T., Taylor, D. R., Perera, W. S., and Hooper, N. M. (2009) alpha-cleavage of the prion protein occurs in a late compartment of the secretory pathway and is independent of lipid rafts. *Mol Cell Neurosci* **40**, 242-248
52. Oliveira-Martins, J. B., Yusa, S., Calella, A. M., Bridel, C., Baumann, F., Dametto, P., and Aguzzi, A. (2010) Unexpected tolerance of alpha-cleavage of the prion protein to sequence variations. *PLoS One* **5**, e9107
53. Lewis, V., Hill, A. F., Haigh, C. L., Klug, G. M., Masters, C. L., Lawson, V. A., and Collins, S. J. (2009) Increased proportions of C1 truncated prion protein protect against cellular M1000 prion infection. *J Neuropathol Exp Neurol* **68**, 1125-1135
54. Seuberlich, T., Gsponer, M., Drogemuller, C., Polak, M. P., McCutcheon, S., Heim, D., Oevermann, A., and Zurbriggen, A. (2012) Novel prion protein in BSE-affected cattle, Switzerland. *Emerg Infect Dis* **18**, 158-159
55. Serra, F., Dudas, S., Torres, J. M., Anderson, R., Oevermann, A., Espinosa, J. C., Czub, S., and Seuberlich, T. (2018) Presumptive BSE cases with an aberrant prion protein phenotype in Switzerland, 2011: Lack of prion disease in experimentally inoculated cattle and bovine prion protein transgenic mice. *Transbound Emerg Dis* **65**, 1348-1356
56. Supattapone, S., Bosque, P., Muramoto, T., Wille, H., Aagaard, C., Peretz, D., Nguyen, H. O., Heinrich, C., Torchia, M., Safar, J., Cohen, F. E., DeArmond, S. J., Prusiner, S. B., and Scott, M. (1999) Prion protein of 106 residues creates an artifical transmission barrier for prion replication in transgenic mice. *Cell* **96**, 869-878
57. Kurt, T. D., Bett, C., Fernandez-Borges, N., Joshi-Barr, S., Hornemann, S., Rulicke, T., Castilla, J., Wuthrich, K., Aguzzi, A., and Sigurdson, C. J. (2014) Prion transmission prevented by modifying the beta2-alpha2 loop structure of host PrPC. *J Neurosci* **34**, 1022-1027
58. Caldarulo, E., Barducci, A., Wuthrich, K., and Parrinello, M. (2017) Prion protein beta2-alpha2 loop conformational landscape. *Proc Natl Acad Sci U S A* **114**, 9617-9622

59. Christen, B., Damberger, F. F., Perez, D. R., Hornemann, S., and Wuthrich, K. (2013) Structural plasticity of the cellular prion protein and implications in health and disease. *Proc Natl Acad Sci U S A* **110**, 8549-8554
60. Choi, J. K., Cali, I., Surewicz, K., Kong, Q., Gambetti, P., and Surewicz, W. K. (2016) Amyloid fibrils from the N-terminal prion protein fragment are infectious. *Proc Natl Acad Sci U S A* **113**, 13851-13856
61. Feraudet, C., Morel, N., Simon, S., Volland, H., Frobert, Y., Creminon, C., Vilette, D., Lehmann, S., and Grassi, J. (2005) Screening of 145 anti-PrP monoclonal antibodies for their capacity to inhibit PrPSc replication in infected cells. *J Biol Chem* **280**, 11247-11258
62. Krasemann, S., Groschup, M., Hunsmann, G., and Bodemer, W. (1996) Induction of antibodies against human prion proteins (PrP) by DNA-mediated immunization of PrP0/0 mice. *J Immunol Methods* **199**, 109-118
63. Langeveld, J. P., Jacobs, J. G., Erkens, J. H., Bossers, A., van Zijderveld, F. G., and van Keulen, L. J. (2006) Rapid and discriminatory diagnosis of scrapie and BSE in retro-pharyngeal lymph nodes of sheep. *BMC Vet Res* **2**, 19
64. Rigter, A., Langeveld, J. P., Timmers-Parohi, D., Jacobs, J. G., Moonen, P. L., and Bossers, A. (2007) Mapping of possible prion protein self-interaction domains using peptide arrays. *BMC Biochem* **8**, 6
65. Pan, T., Chang, B., Wong, P., Li, C., Li, R., Kang, S. C., Robinson, J. D., Thompsett, A. R., Tein, P., Yin, S., Barnard, G., McConnell, I., Brown, D. R., Wisniewski, T., and Sy, M. S. (2005) An aggregation-specific enzyme-linked immunosorbent assay: detection of conformational differences between recombinant PrP protein dimers and PrP(Sc) aggregates. *J Virol* **79**, 12355-12364
66. Vilotte, J. L., Soulier, S., Essalmani, R., Stinnakre, M. G., Vaiman, D., Lepourry, L., Da Silva, J. C., Besnard, N., Dawson, M., Buschmann, A., Groschup, M., Petit, S., Madelaine, M. F., Rakatobe, S., Le Dur, A., Vilette, D., and Laude, H. (2001) Markedly increased susceptibility to natural sheep scrapie of transgenic mice expressing ovine prp. *J Virol* **75**, 5977-5984
67. Langevin, C., Andreoletti, O., Le Dur, A., Laude, H., and Beringue, V. (2011) Marked influence of the route of infection on prion strain apparent phenotype in a scrapie transgenic mouse model. *Neurobiol Dis* **41**, 219-225
68. Salamat, K., Moudjou, M., Chapuis, J., Herzog, L., Jaumain, E., Beringue, V., Rezaei, H., Pastore, A., Laude, H., and Dron, M. (2012) Integrity of helix 2-helix 3 domain of the PrP protein is not mandatory for prion replication. *J Biol Chem* **287**, 18953-18964
69. Dron, M., Moudjou, M., Chapuis, J., Salamat, M. K., Bernard, J., Cronier, S., Langevin, C., and Laude, H. (2010) Endogenous proteolytic cleavage of disease-associated prion protein to produce C2 fragments is strongly cell- and tissue-dependent. *J Biol Chem* **285**, 10252-10264
70. Dron, M., Dandoy-Dron, F., Farooq Salamat, M. K., and Laude, H. (2009) Proteasome inhibitors promote the sequestration of PrPSc into aggresomes within the cytosol of prion-infected CAD neuronal cells. *J Gen Virol* **90**, 2050-2060
71. Shen, Y., and Bax, A. (2013) Protein backbone and sidechain torsion angles predicted from NMR chemical shifts using artificial neural networks. *J Biomol NMR* **56**, 227-241
72. Grzela, R., Nusbaum, J., Fieulaine, S., Lavecchia, F., Desmadril, M., Nhiri, N., Van Dorsselaer, A., Cianferani, S., Jacquet, E., Meinnel, T., and Giglione, C. (2018) Peptide deformylases from Vibrio parahaemolyticus phage and bacteria display similar deformylase activity and inhibitor binding clefts. *Biochim Biophys Acta Proteins Proteom* **1866**, 348-355
73. Gielbert, A., Davis, L. A., Sayers, A. R., Hope, J., Gill, A. C., and Sauer, M. J. (2009) High-resolution differentiation of transmissible spongiform encephalopathy strains by quantitative N-terminal amino acid profiling (N-TAAP) of PK-digested abnormal prion protein. *J Mass Spectrom* **44**, 384-396

74. Westaway, D., Goodman, P. A., Mirenda, C. A., McKinley, M. P., Carlson, G. A., and Prusiner, S. B. (1987) Distinct prion proteins in short and long scrapie incubation period mice. *Cell* **51**, 651-662
75. Barron, R. M., Baybutt, H., Tuzi, N. L., McCormack, J., King, D., Moore, R. C., Melton, D. W., and Manson, J. C. (2005) Polymorphisms at codons 108 and 189 in murine PrP play distinct roles in the control of scrapie incubation time. *J Gen Virol* **86**, 859-868

Figures

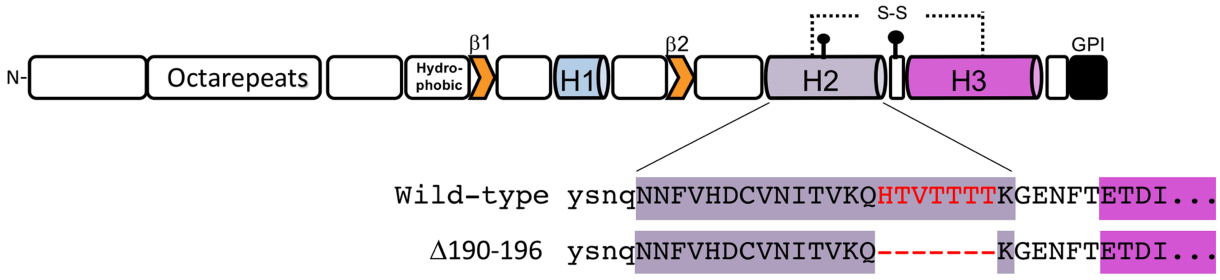

Figure 1. Δ190-196 PrP sequence. On the top is the schematic representation of mature ovine PrP^{C} (23 to 234). Secondary structures building the globular part of the protein, the two short beta strands forming a beta sheet and the three alpha-helices are indicated. Post-translational modifications such as N-glycan chains (black dots), disulfide bridge (S-S) and the GPI anchor are also shown. Below, the amino acid sequence of alpha-helix H2 is highlighted in lavender color and the first residues of H3 in purple. Residues 190-196 that were removed from the WT PrP are colored in red and replaced by a dotted line for the deletion mutant.

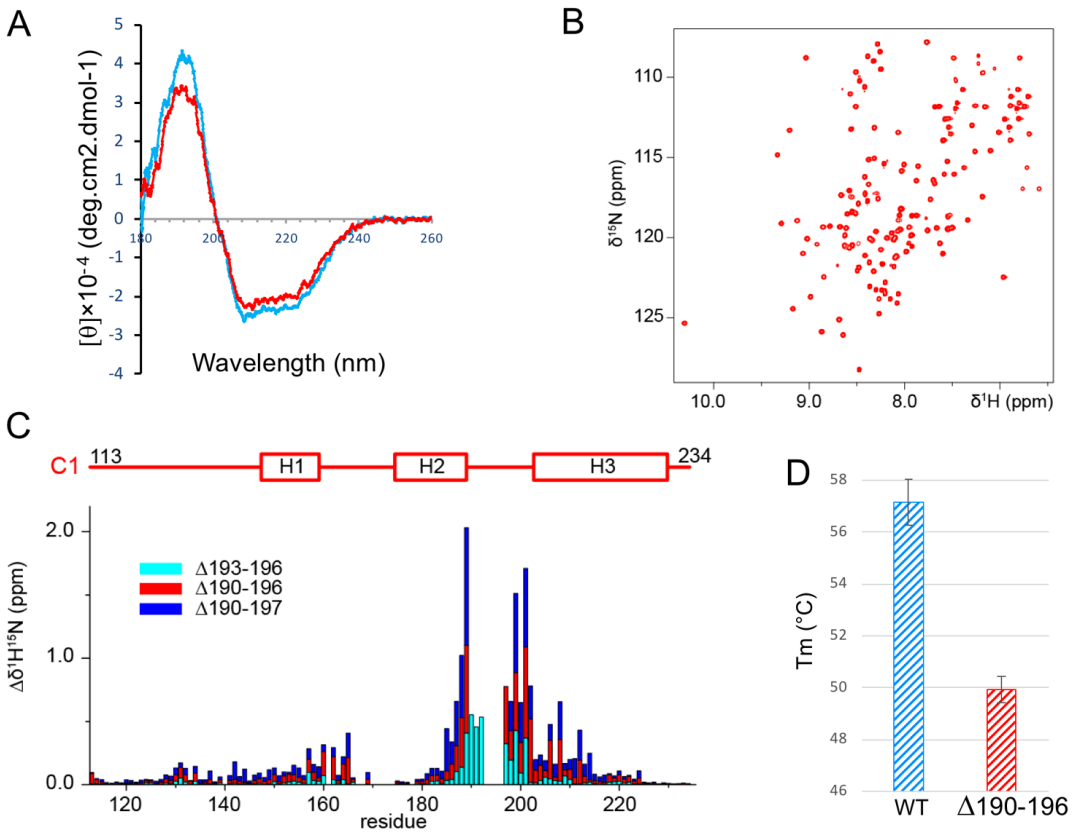

Figure 2. Structure and stability of recombinant Δ190-196 PrP. **A.** Comparative analysis of the secondary structures of WT PrP (blue) and Δ190-196 PrP (red) by circular dichroism. Far UV spectra indicate that the secondary structure of full-length WT PrP is essentially maintained in the mutant protein. **B.** NMR spectroscopy analysis of the C1-like segment (113-234) of Δ190-196 mutant PrP. 2D ^{1}H-^{15}N HSQC spectrum of 250 µM recombinant ^{15}N^{13}C-labeled Δ190-196 $C1_{113}$, acquired at a magnetic field of 18.8 T and a temperature of 298 K. **C.** Combined amide chemical perturbations (obtained with weighing factors of 1 for ^{1}H and 1/10 for ^{15}N), measured for each non-proline residue with respect to WT PrP, are represented as superimposed bar diagrams. Perturbations are shown for Δ190-196 $C1_{113}$ (red color) and compared to those previously obtained for PrP Δ193-196 (cyan) and Δ190-197 (blue) (23,24). The position of the three alpha-helices H1, H2 and H3, obtained by analysis of Δ190-196 $C1_{113}$ ^{13}Calpha chemical shifts by TALOS-N (71) is shown above. **D.** Comparison of stability between WT and Δ190-196 mutant PrP. Means melting temperatures (Tm) and standard deviations from 5 experiments were determined for full-length WT PrP (blue, 57.1 °C ± 0.9 °C) and Δ190-196 PrP (red, 49.9 °C ± 0.5 °C), for proteins resuspended in the same buffer conditions as for CD and NMR analysis (Na acetate 10mM, pH5).

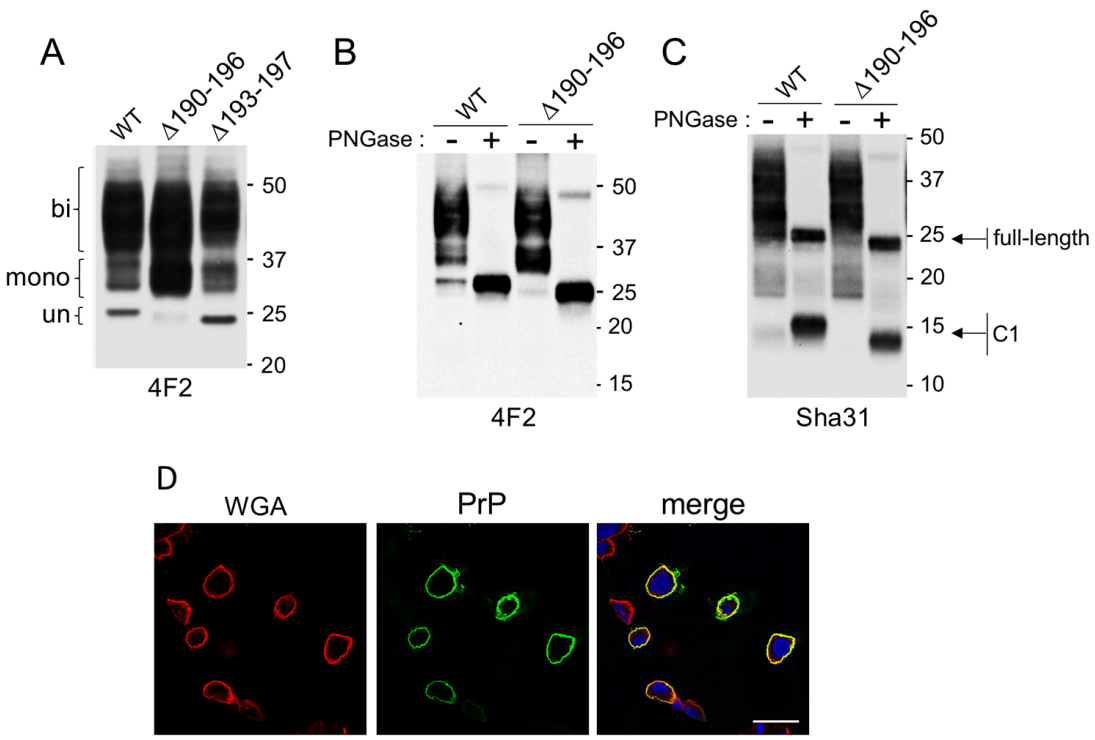

Figure 3. Expression of WT and Δ190-196 PrP^C in RK13 cells. **A.** Comparison of the electrophoretic profile of WT PrP, Δ190-196 mutant PrP and the previously established closely related Δ193-197 mutant (23) by immunoblotting. Molecular-weight size markers are indicated on the right of panel. On the left, un- , mono- and bi-glycosylated species are indicated. **B.** and **C.** PNGase F treatment was used to resolve the PrP pattern as a single aglycosylated polypeptide. **D.** confocal microscopy analysis of immunostained cells showed colocalization (merge; in yellow) of Δ190-196 PrP (green) with WGA (red) at the cell surface; bar 50µm. The 4F2 anti-PrP mAb was used in **A.**, **B.** and **D.** and Sha31 mAb for **C.**

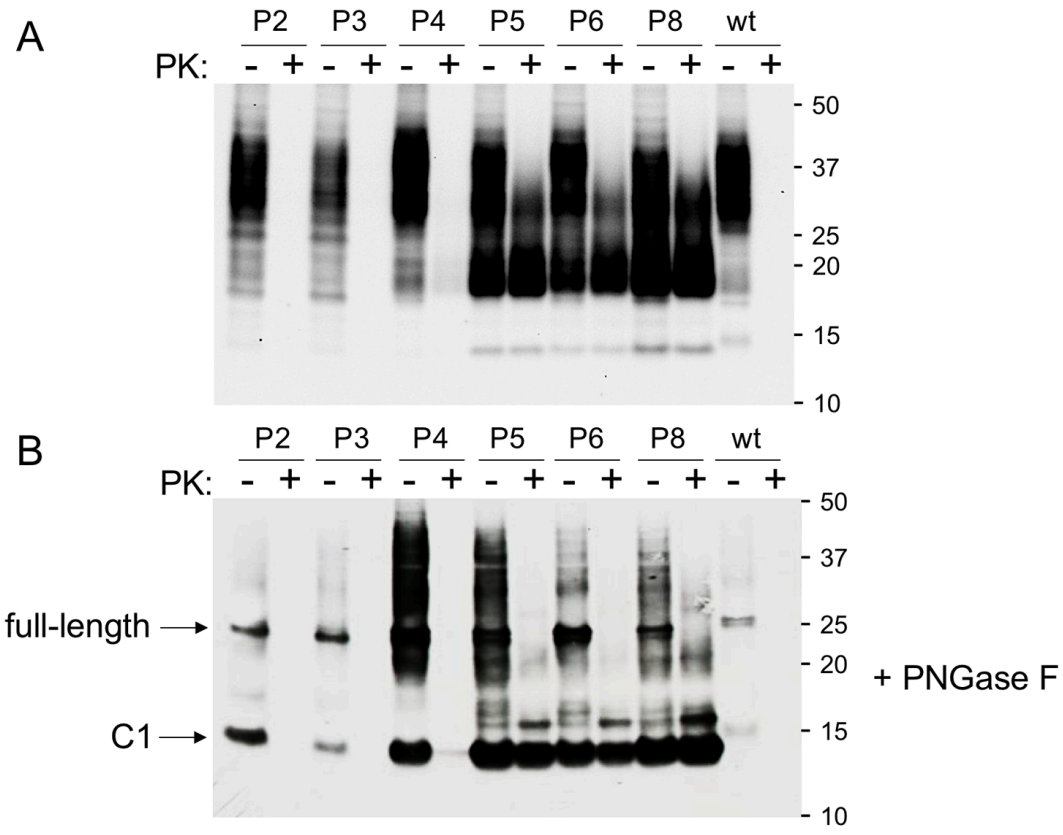

Figure 4. Spontaneous formation of PK-resistant PrP in Δ190-196 Rov cells. Immunoblots of samples from Δ190-196 Rov cell cultures over passaging, 2th to 8 th passage (P2 – P8), as indicated at the top of each panel. **A.** The equivalent of 10µg of total protein from the cellular lysates were treated or not with PK as indicated at the top of lanes, and were loaded on the gel. **B.** The same samples than in the upper blot were treated with PNGase F before loading. Full- length mutant PrPs and the C1 fragments are indicated by an arrow. Immunoblots were done with Sha31 mAb.

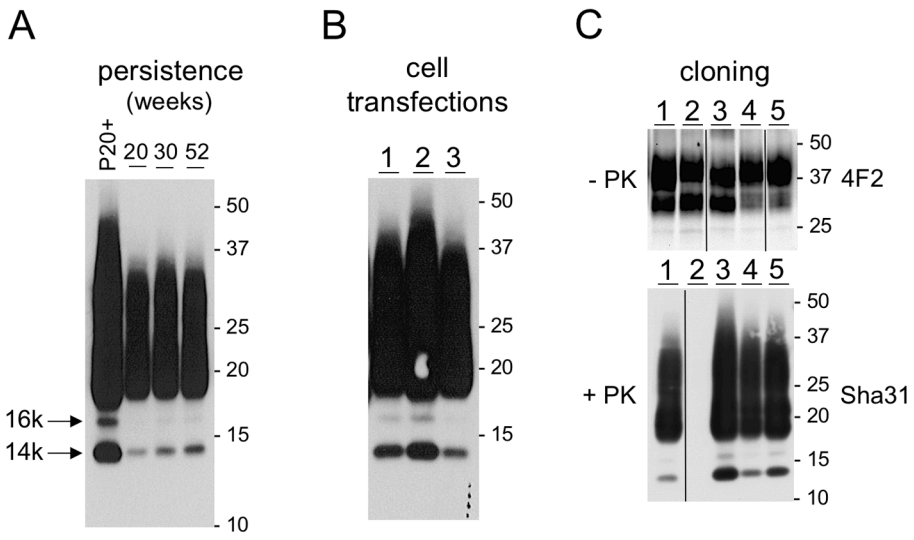

Figure 5. Persistence of the PK-resistant form in cultures, insolubility of PrP^{res} and reproducibility of spontaneous conversion. Immunoblots of PK-treated samples are shown. **A.** Δ190-196 PrP^{Sc} was produced persistently up to one year of continuous cell culture passage (1 per week). PrP^{res} at 20, 30 and 52 weeks of culture are shown: 10µg of total protein in 10µl of cell lysate were digested and loaded (lanes 2 to 4). In lane 1 (P20+), the equivalent of 100µg of protein from the passage at 20 weeks was loaded after PK digestion and concentration of insoluble material at 22,000 x g, to improve detection of the 14 kDa and 16 kDa unglycosylated bands (Sha31 mAb). **B.** Spontaneous emergence of Δ190-196 PrP^{res} in three populations of Δ190-196 Rov cells obtained from independent transfections (lanes 1 to 3). **C.** Individual clones isolated from two independent transfections. Five clones (lanes 1 to 5) with roughly similar Δ190-196 PrP expression levels (upper panel, 4F2 mAb) are shown. They produced spontaneously the PK-resistant form after eight passages of culture (lanes 1, 3, 4, 5) with the exception of clone 12 (lane 2) (lower panel, Sha31 mAb).

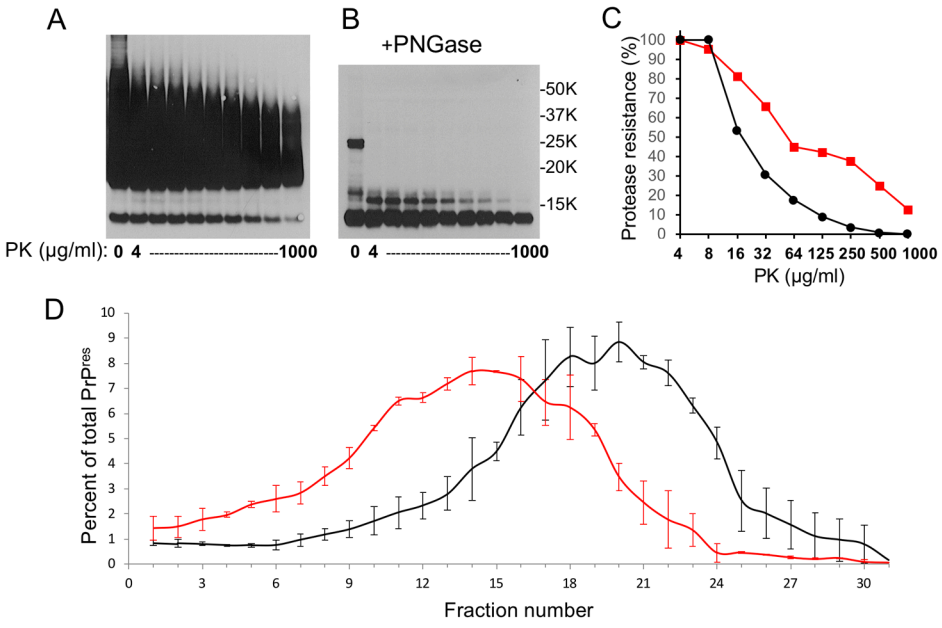

Figure 6. PK-resistance and aggregation state of Δ190-196 PrP^{res}. **A.** Δ190-196 PrP^{res} resists to high concentrations of PK. 10µg of total protein were treated with two-fold increasing concentrations of PK up to 1mg/ml. **B.** Samples obtained in **A** were treated with PNGase F to visualize and determine the molecular weight of polypeptides after PK treatment. **C.** Comparative PK-resistance of Δ190-196 PrP^{Sc} (red squares) and 127S PrP^{Sc} (dark dots). **D.** Sedimentation velocity profile of Δ190-196 PrP^{Sc} (red lane) and 127S PrP^{Sc} (dark lane). Fraction number 1 corresponds to the top of the gradient. Results are the means ± SD of three independent experiments. In **C** and **D,** both proteins were extracted from uninfected Δ190-196 Rov cells and 127S-infected Rov cells, respectively.

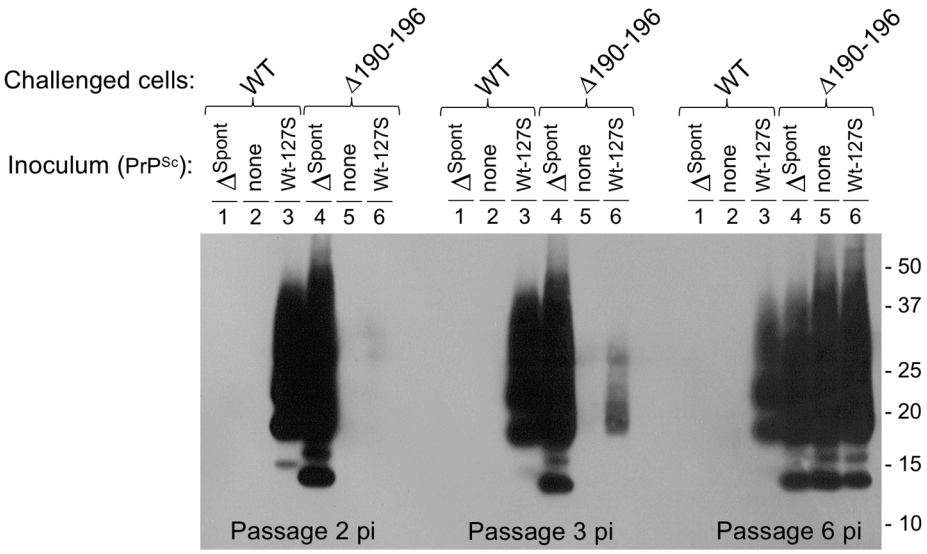

Figure 7. Infectious potential of Δ^{Spont} prions. Rov cells expressing either WT PrP or Δ190-196 PrP were challenged with cell homogenates from Δ190-196 Rov cells (Δ^{Spont} inoculum), 127S-infected WT Rov cells (WT-127S) or non-infected RK13 cells (none). Cells were analyzed for presence of PK-resistant PrP from passage 2 to 6 post-infection, as indicated. Western blot was done with Sha31 mAb.

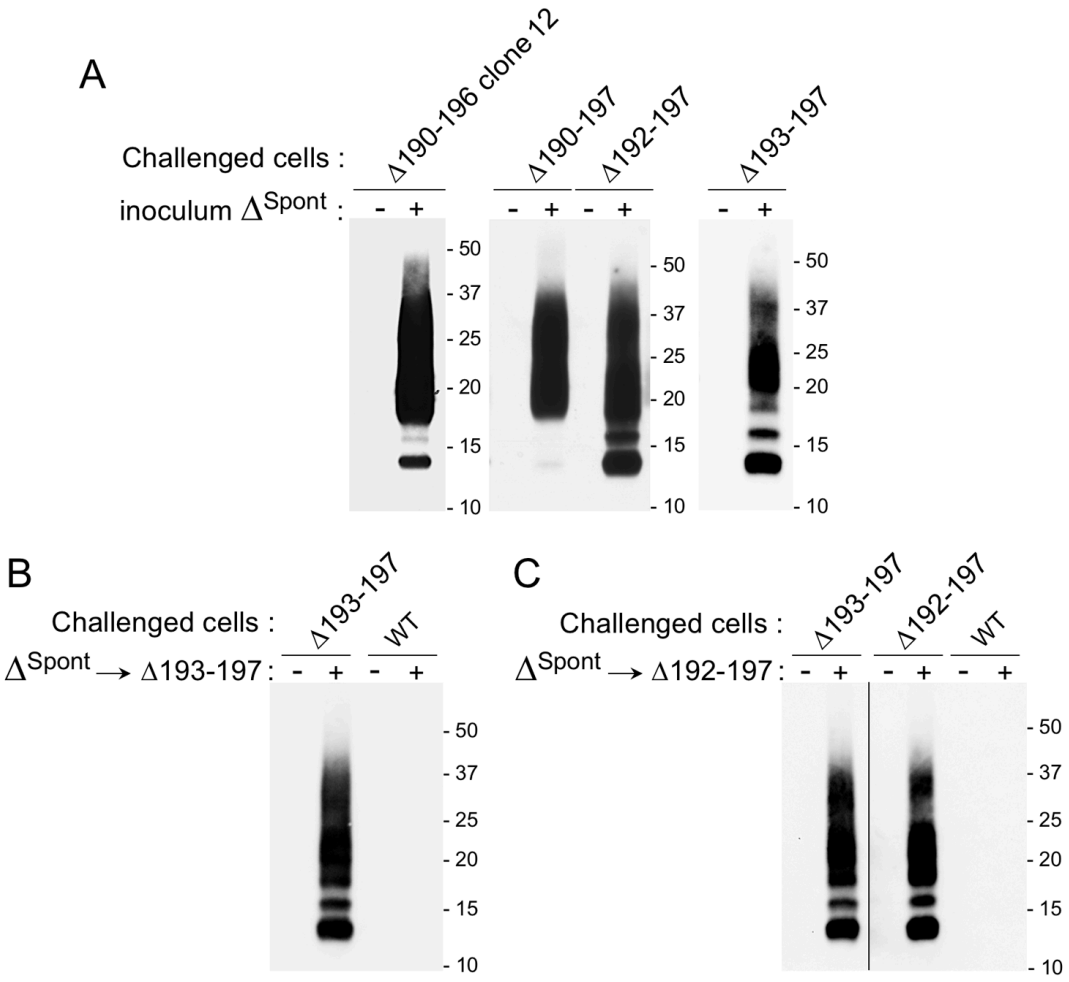

Figure 8. Conversion of homologous PrP or closely related mutant PrPs by Δ^{Spont} prions. **A.** Δ190-196 Rov clone 12 that did not produce spontaneously Δ^{Spont} PrP^{res} was infected by Δ^{Spont} prions (left panel). Rov cells expressing other closely related deletion mutants were also susceptible to the infection by Δ^{Spont} prions (middle and right panel). Immunoblots show PK-treated samples, 8 passages post-infection. **B.** Cell homogenates of Δ193-197 or Δ192-197 Rov cells inoculated with Δ^{Spont} prions (8^{th} passage, ($\Delta^{Spont} \rightarrow$ Δ193-197 and $\Delta^{Spont} \rightarrow$ Δ192-197) were used as inocula to infect Rov cells expressing homologous PrP, WT PrP or the other mutant. The analysis of PK-treated samples harvested after 8 passages post-infection is shown.

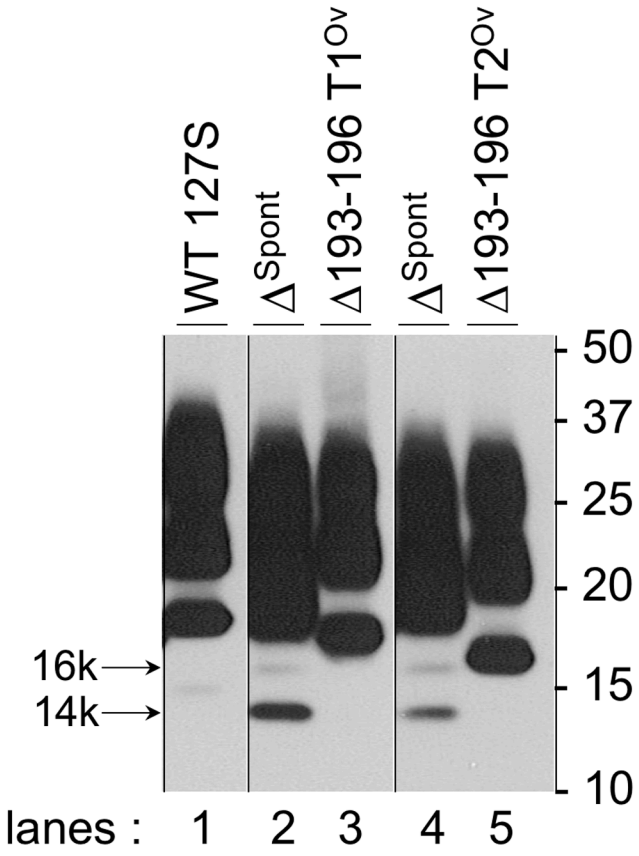

Figure 9. Molecular typing of Δ^{Spont} PrP^{res}. The electrophoretic profiles of prions propagated on Rov cells were compared. The profile of Δ^{Spont} PrP^{res} (lanes 2 and 4) with its 14 kDa and 16 kDa bands, as indicated by an arrow, was different from those of type1 strains (127S and $T1^{ov}$, lane 1 and 3, respectively) and type 2 strain ($T2^{Ov}$, lane 5) propagated in WT Rov (lane 1) or in Δ193-196 Rov cells (lanes 3 and 5).

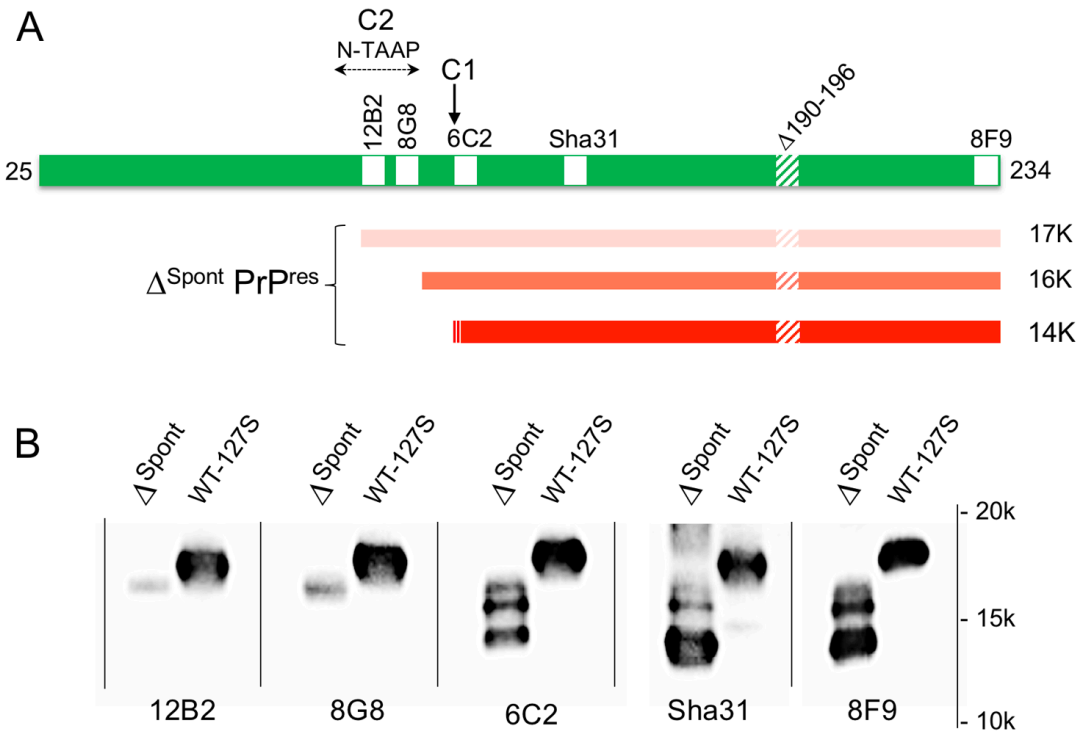

Figure 10. Epitope mapping of Δ^{Spont} PrP^{res}. **A.** Scheme representing mature ovine PrP (25 to 234, in green) with name and position of mAbs epitopes (open square). The alpha cleavage site generating C1 fragment is indicated by an arrow. The area covering N-terminal amino acid profile (N-TAAP) variations of C2 PrP^{res} fragments among prion strains (73) is indicated by horizontal double arrow dotted line. PrP^{res} fragments resulting from PK digestion of Δ^{Spont} prions are represented below the scheme, the 14kDa C1-like PrP^{res} is in red, the 16kDa in orange and the faint 17kDa C2-like species in pink. **B.** Representative western blots of PNGase F-treated Δ^{Spont} PrP^{res} and WT PrP^{res} revealed with the different anti-PrP mAbs. For the comparative analysis, the same couple of PrP^{res} samples was loaded several times on a same gel, separated by stained molecular-weight markers and then transferred on a membrane that was split into six parts, each being incubated with a different primary antibody, as indicated.

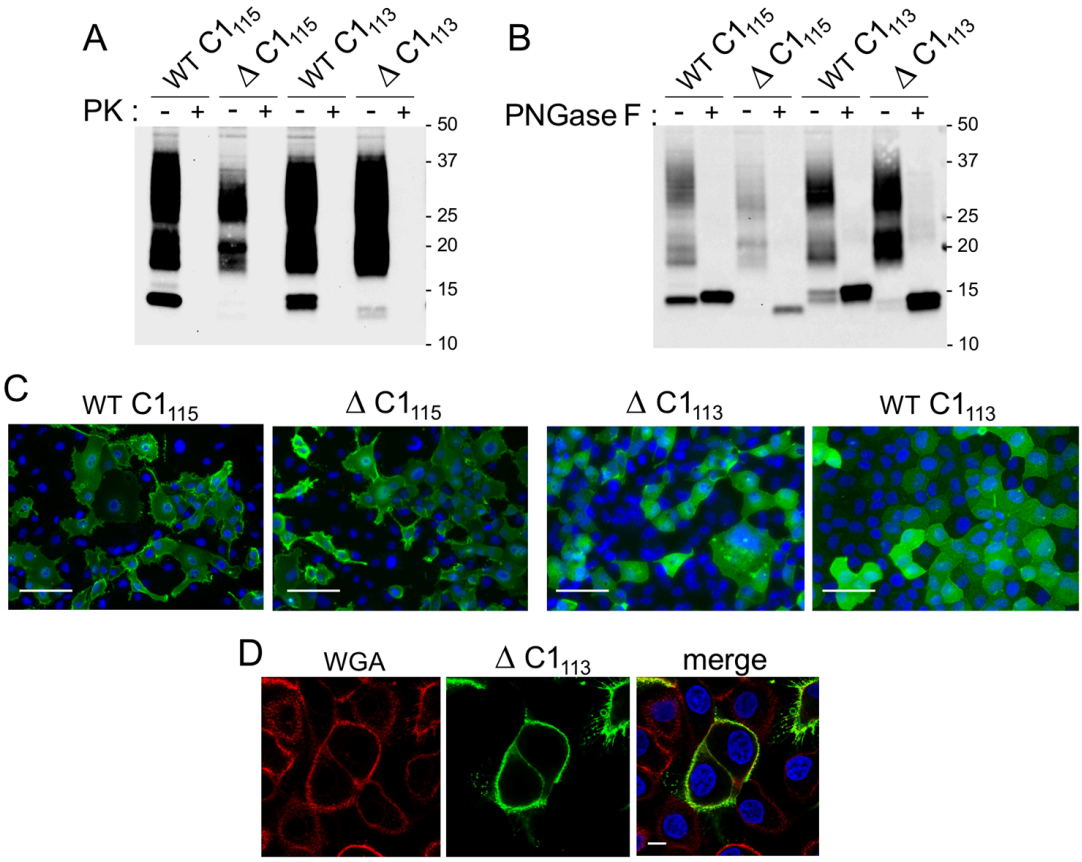

Figure 11. Expression of WT and Δ190-196 C1 polypeptides in RK13 cells. **A.** Immunoblot analysis of stably transfected C1 constructs, before or after PK treatment. The expression of C1-like polypeptides (residues 113-234 and 115-234 of ovine PrP, $C1_{113}$ and $C1_{115}$, respectively) and equivalent fragments with the HTVTTTT Δ190-196 deletion ($\Delta C1_{113}$ and $\Delta C1_{115}$) was analyzed. **B.** Immunoblot analysis of the same C1 constructs before and after PNGase F treatment. 25µg of cellular protein was loaded. **C.** C1 PrP^C expression pattern by immunofluorescence. PrP^C (green) and nuclear marker 4',6-diamidino-2-phenylindole (DAPI, blue) staining of non-permeabilized fixed cells. Scale bars 50µM. **D.** Confocal microscopy imaging of $\Delta C1_{113}$ Rov cells co-stained for white germ agglutinin (WGA, red) and PrP (green). Nuclei are stained with DAPI (blue). Merged confocal images or individual channels are shown. Scale bar 10µM.

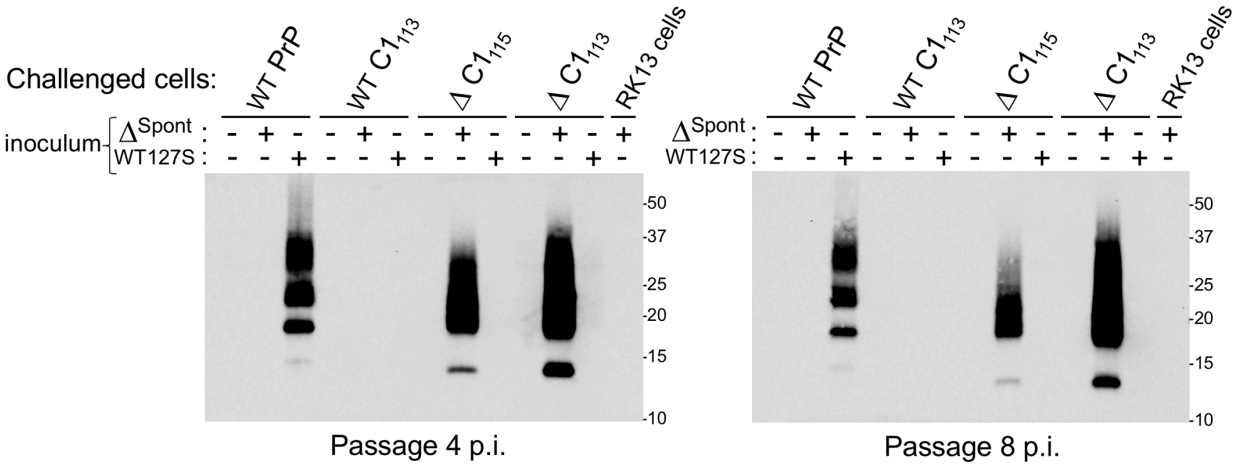

Figure 12. Infection of WT C1 and ΔC1 Rov cells by 127S or Δ^{Spont} prions. Immunoblots of PK-treated samples at passage 4 (left) or passage 8 (right) post-infections are shown. Sha31 mAb defines both $C1_{113}$ and $C1_{115}$.

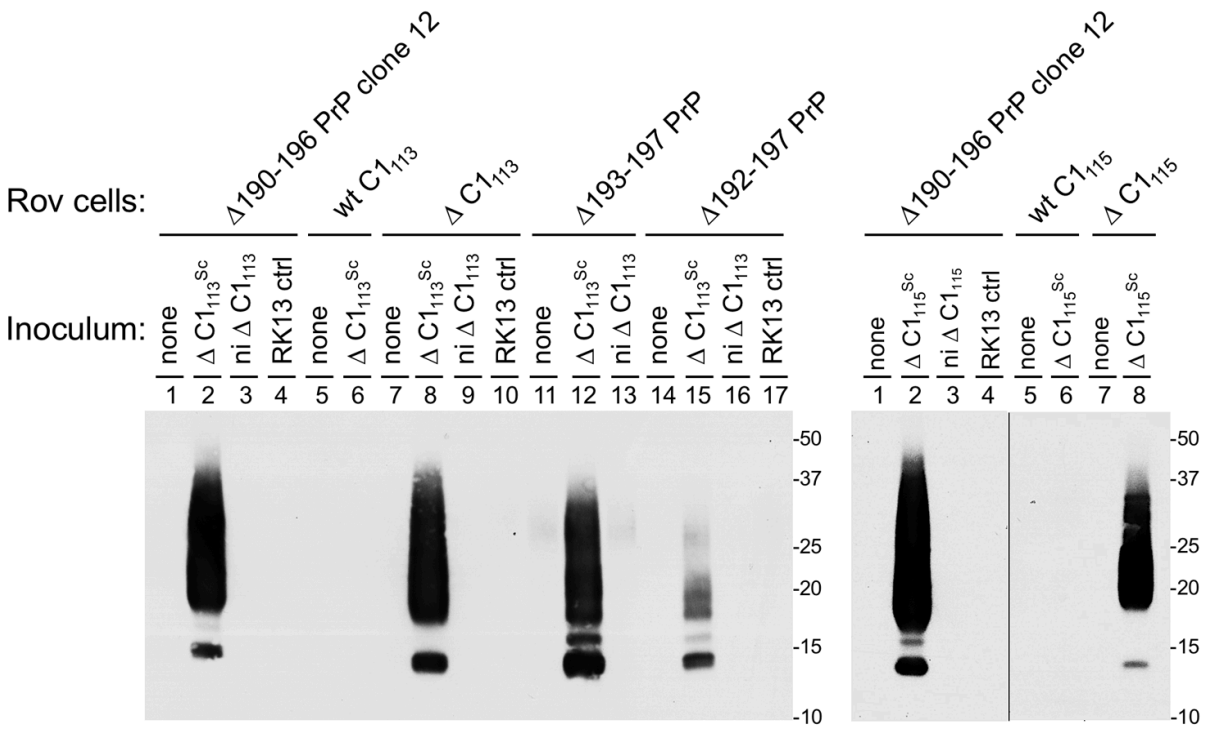

Figure 13. Infectivity of $\Delta C1^{Sc}$ prions. Rov cells expressing different forms of mutated, full-length PrP and WT/mutated C1 PrP were left uninfected (none) or exposed to $\Delta C1^{Sc}$ (left panel, $\Delta C1_{113}^{Sc}$; right panel $\Delta C1_{115}^{Sc}$) obtained from cell homogenates at passage 8 (see figure 11). As controls, non-infected cells (ni $\Delta C1_{113}$, ni $\Delta C1_{115}$) and Δ^{Spont}-infected RK13 cells (RK13 ctrl) were used. The challenged cells were Δ190-196 Rov cell clone 12 that did not produce spontaneously Δ^{Spont} prions, Rov cells expressing closely related full-length deletion mutants (Δ193-197, Δ192-196), populations of cells expressing either WT or Δ version of $C1_{113}$ ($\Delta C1_{113}$) and of $C1_{115}$ ($\Delta C1_{115}$). Immunoblots of PK-treated cell lysates at passage 8 post-infection are shown (Sha31 mAb).

---A seven-residue deletion in PrP leads to generation of a spontaneous prion formed from C-terminal C1 fragment of PrP

Carola Munoz-Montesino, Djabir Larkem, Clément Barbereau, Angélique Igel-Egalon, Sandrine Truchet, Eric Jacquet, Naïma Nhiri, Mohammed Moudjou, Christina Sizun, Human Rezaei, Vincent Béringue and Michel Dron

J. Biol. Chem. published online August 11, 2020

Access the most updated version of this article at doi: 10.1074/jbc.RA120.014738